Building connectomes using diffusion MRI: Why, how and but

Stamatios N Sotiropoulos[1,2] & Andrew Zalesky[3]

[1]Centre for Functional MRI of the Brain (FMRIB), Nuffield Department of Clinical Neurosciences, University of Oxford, Oxford, UK
[2]Sir Peter Mansfield Imaging Centre, School of Medicine, University of Nottingham, Nottingham, UK
[3]Melbourne Neuropsychiatry Centre and Melbourne School of Engineering, University of Melbourne, Victoria, Australia

Abstract

Why has diffusion MRI become a principal modality for mapping connectomes in vivo? How do different image acquisition parameters, fiber tracking algorithms and other methodological choices affect connectome estimation? What are the main factors that dictate the success and failure of connectome reconstruction? These are some of the key questions that we aim to address in this review. We provide an overview of the key methods that can be used to estimate the nodes and edges of macroscale connectomes, and we discuss open problems and inherent limitations. We argue that diffusion MRI-based connectome mapping methods are still in their infancy and caution against blind application of deep white matter tractography due to the challenges inherent to connectome reconstruction. We review a number of studies that provide evidence of useful microstructural and network properties that can be extracted in various independent and biologically-relevant contexts. Finally, we highlight some of the key deficiencies of current macroscale connectome mapping methodologies and motivate future developments.

Introduction

Functional integration, the interaction and information transfer between different subunits in the brain, is mediated in part through white matter connections [1]. The formation of these fiber pathways is guided by genetic, but also environmental factors. During the early phases of development, an initial over-production of synapses is followed by pruning of the redundant connections in response to first life experiences [2]. The continuous maturation and myelination of white matter from the first months of life and through to adulthood reflects learning and interactions with external stimuli.

This experience-dependent molding of brain connectivity [3] sheds light on the functional relevance of white matter pathways. Anatomical connections constrain neural computations. In fact, the pattern of anatomical connections a brain region has with other regions can predict, to a certain extent, the function of that region at a systems level [4, 5]. This notion of connectivity fingerprinting and its functional implications has increased interest in studying connections and structural organization [6]. The term *connectome*, proposed roughly ten years ago [7, 8], describes a comprehensive network map of extrinsic connections between functionally specialized brain regions. Ideally, such a map does not only contain a list of connected areas, but also the relative strengths and directionality of each connection [8]. Connectomics has the potential to reveal new insights into the principles that guide how different functional subunits are arranged and influence one another [9] as well as how these processes are perturbed in pathological brain conditions [10].

Invasive approaches for mapping brain connections have existed for many decades [11]. At the microscale, techniques such as automated histological staining [12, 13], serial electron microscopy [14] and 3D fluorescence imaging [15] allow more data to be collected and processed nowadays with less labor-intensive methods and fewer imaging distortions. However, the small field of view of microscopy techniques limits their applicability to small model species, such as the nematode C. Elegans [16], and mapping exquisite details of small tissue segments in larger species. At the mesoscale, chemical tracers are considered to be the gold standard for mapping longer-range white matter connections as they allow very high measurement accuracy and detail. In fact, the majority of our knowledge on white matter organisation has been obtained through tracer studies (see [17] for a review) and macroscopic connectome matrices for different animals and scales have been obtained (for instance [18-23]).

Non-invasive imaging techniques offer an alternative modality for connectome reconstruction at the macroscale in living humans [17]. Diffusion MRI and tractography techniques (see other review papers in this issue) have been successfully used for many years now to reconstruct the trajectories and estimate microstructural properties of fiber bundles in white matter [24]. In comparison to invasive approaches, these methods are indirect; they do not

explicitly measure the quantity of interest, but rather rely on models and inference. For this reason, they are error prone and the results can be more difficult to quantify compared to corresponding invasive methods [25]. They also offer substantially lower spatial resolution than chemical tracers and microscopic techniques and they cannot estimate the directionality of connections. However, in-vivo mapping of connections in humans offers the potential of considerable advantages [6]: 1) many connections in many subjects can be studied simultaneously, 2) structural connections can be mapped along with function, behavior and genetics and 3) changes in connections with development, aging or pathology can be probed.

In this review we consider existing methodologies for mapping the connectome using diffusion MRI (dMRI). We discuss the impact on connectome reconstruction of different image acquisition parameters, fiber tracking algorithms and other methodological choices. We highlight comparative and validation studies that provide evidence for the potential of these methods but also reveal their deficiencies. Furthermore, we consider features of white matter connectivity that are inherently difficult to reconstruct with existing approaches. Such features impose limits on the biological specificity of dMRI-derived quantities and motivate new developments and shifts in current connectivity mapping paradigms.

Building a connectome

In-vivo MRI methods provide a *macroscopic* view of the connectome. Connections that can be reconstructed with dMRI and tractography are the extrinsic[†] pathways between regions that traverse white matter. Even if these constitute only a small fraction (~10%) of the total number of neuronal connections [26] (the others are intrinsic, intra-cortical), they are important to study in order to understand the brain at the level of a system and they are characterized by considerable complexity (see [27] for a review of these complex features).

Inferring a *macro*-connectome from dMRI images is a very challenging task and a field of active research. We divide connectome mapping into two tasks: node delineation and edge mapping (Figure 1). Nodes represent spatially distinct cortical and subcortical gray matter regions, while edges represent the white matter fiber bundles that interconnect pairs of regions.

Node delineation

Specifying a parcellation scheme that subdivides cortical and subcortical gray matter into discrete, spatially contiguous parcels is not straightforward [28]. Architectonic atlases provide the simplest and perhaps most commonly used approach. Many such atlases are available (see [29] for a review) and they can be registered to an individual brain to ensure that nodes between subjects are matched with respect to average size, geometry and location. However, architectonic and other template-based atlases do not capture variation between individuals in regional functional boundaries and thus make the simplifying assumption that a common parcellation is representative of all individuals. For instance, the AAL [30] and Harvard-Oxford [31] atlases are based on anatomical landmarks, while the parcellation of the Talairach Daemon [32] and the Juelich atlas [33] are based on cytoarchitectonic features from post-mortem brains.

Data-driven parcellations offer an individually customised alternative. Data from task-based or resting-state functional MRI can be used to define areas with homogeneous features across a population comprising hundreds of subjects [34-38]. In this way, regions are delineated based on functional properties that are specific to the individuals for whom connectomes are to be

---

[†] Extrinsic [4, 9] connections that traverse white-matter include local U-fibres (up to ~30 mm in length) connecting neighbouring regions and long-range fascicles connecting remote regions within or between hemispheres. Intrinsic connections are horizontal intra-cortical (<3 mm in length). It is estimated that the number of intrinsic connections (~10^{11} fibres) is an order of magnitude larger than the number of U-fibres (~10^{10}). U-fibres are an order of magnitude more than long-range connections (~10^9 fibres) [26]. Even if extrinsic connections are considerably less than the intrinsic ones, they provide the network links necessary to achieve functional integration.

mapped. Methods for defining functional boundaries are many and varied, with the most recent utilizing multiple modalities and unique measurements. For instance, [39] uses multiple features simultaneously, such as cortical folding, myelin content, resting-state and task-based activity, to identify a functionally-relevant and population-specific parcellation, which respects individual variability. In [40], the authors use structural, functional and behavioral features to identify a parcellation consistent across various domains.

Limitations and open problems

Diffusion MRI and tractography methods can be also used to extract connection patterns and probe functional boundaries [4, 9]. This has been shown with controlled studies for a large number of regions in the cortex and subcortex (for instance [41-44], see also the "Validation-Indirect Evidence" section). However, current limitations in structural connectome estimation, as we explore throughout this Review, can limit the accuracy, interpretability and generalizability of such approaches for node delineation.

While parcellating the cortex based on functional homogeneity is an attractive alternative to node delineation, it also suffers from methodological caveats [45]. Furthermore, a number of conceptual problems exist with respect to the definition of areal boundaries [46]. Here, we briefly review some of these considerations.

Individual variability

Individual variability in brain function and structure complicates the interpretability of population-level parcellations. Well-characterised areas, such as V1, can vary in areal size by 2-fold across subjects [46, 47]. The relationship between functional boundaries and cortical folding is also highly variable. Areas associated with high-order function exhibit more variability across subjects in folding patterns than primary areas, where the folds can be reasonable predictors of the boundaries [48]. Therefore, a group-level parcellation template cannot capture subtle yet important variations between individuals. Registration frameworks that align functional features rather than simply match geometry or cortical folding could offer a way to approach this problem [49].

Within-region heterogeneity

Different patterns can characterise the functional and topographical organization of a region. For instance, different within-area topographical organisation can underlie different functions of the same region [50]. V1 and V2 provide such examples, with their central and peripheral subregions exhibiting different relationships with other regions of the cortex [46]. This within-area heterogeneity, along with individual variability, makes delineation of boundaries very challenging. A potential solution is to define smooth

transitions and fuzzy boundaries between regions rather than binary parcellations. But that fuzziness should reflect uncertainty in functional features rather than data noise, folding differences or alignment errors.

Scale and number of nodes

In many studies, the coarseness of gray matter subdivisions is a relatively arbitrary choice. Principled data-driven methods to perform model selection and define an optimal number of nodes exist for parcellations based on functional data [37]. However, these methods may be conflicted by the tradeoff between true functional relevance and discriminative power of the available data. For instance, using fMRI versus MEG data is accompanied with different limitations in spatial and temporal resolution, which can influence model selection. For this reason, some investigators have resorted to multi-scale schemes to ensure findings are generalizable and not sensitive to a given parcellation resolution [51, 52].

The coarseness of a node parcellation influences the process of mapping white matter connections. In practice, edge mapping and node delineation are performed independently and the outputs of these two processes are only combined when mapping a connectivity matrix. Parcellations with fewer regions tend to give more reproducible and "smooth" mappings than finer ones, whereas more detailed parcellations in principle preserve more details [53, 54]. Low to mid-scale parcellations (in the order of tens to a few hundred regions) have been shown to increase agreement of dMRI-estimated connectomes with tracers in the mouse [55, 56] and monkey brain [57], when compared to results from finer subdivisions.

In *summary*, methods for delineating connectome nodes are many and varied. The number of nodes and specific nodal parcellation that is best suited to a given application is usually not obvious. Parcellations that are informed by both brain anatomy and/or functional specialization have gained significant traction in the field. In the future, parcellation strategies should be developed that capture individual variability. Unlike the microscale, where the parallel between nodes and neurons is obvious, defining nodes at the macroscale is less clear. It is therefore wise to assess the consistency of results for a coarse anatomical parcellation as well as a finer parcellation that is delineated functionally or perhaps randomly. Inconsistencies that emerge between these two scales can potentially shed light on the nature of a particular finding.

Mapping edges

Once the nodes of a connectome have been defined, tractography can be used to estimate edges - the connecting paths between pairs of regions.

While other indirect methods exist [17, 58], diffusion MRI-based tractography is the only method that allows localization of white matter bundles in-vivo (see [59, 60] and papers in this special issue for reviews). Axonal fiber bundles are organized coherently such that water diffusion occurs preferentially along the orientations of least hindrance, which are typically parallel to the fibers. In contrast, diffusion is maximally hindered in the perpendicular direction. The preferred diffusion orientations (PDOs) can be indirectly mapped to fiber orientations at a voxel-wise level (see [61, 62] and papers in this special issue for reviews). Tractography approaches then integrate the voxel-wise information at a global scale and propagate curves that are maximally tangential to the local PDOs [63]. These curves provide estimates of the white matter bundles [64].

There is a plethora of methods for mapping fiber orientations and for curve propagation. The diffusion tensor model [65] is the simplest approach and provides a unimodal approximation to the underlying fiber configurations. A more accurate model in the case of complex fiber patterns is the fiber orientation density function (fODF), which characterizes the fiber distribution in each voxel. Deconvolution methods, parametric [42, 66-68] or non-parametric [69-71], q-ball imaging [72] and diffusion spectrum imaging [73] are some of the popular methods that can provide estimates of the fODF[‡] and a discrete number of crossing orientations in each voxel. The importance in estimating crossings and the maturity of deconvolution methods have been shown in many instances for tracking deep white matter[§] (e.g. [73-78]). A recent study showed benefits of considering fODFs for tracking into the transition from WM to GM [79].

Tractography methods can be grouped into two categories: a) Local approaches [63, 80-82], which in a greedy, step-by-step fashion propagate curves (or streamlines) that are tangent to vector fields extracted from the fODFs. b) Global methods (for instance [83-89]), which estimate paths that are optimal according to a global criterion. Such paths are not necessarily tangent at every point of their route to the local fODF/vector fields. In principle, they are more immune to local errors. Local methods have been by far the most popular and applied approaches. Global methods offer a promising alternative [77, 90], but they require further validation, and they can be more cumbersome and computationally demanding. Global methods have been tested mostly for deep white matter tracking, and thus the extent to which they share or solve some of the limitations and open problems local methods have for connectome mapping (see next section) is yet to be explored.

[‡] Strictly speaking, q-ball and diffusion spectrum imaging provide an estimate of the diffusion ODF, a blurred version of the fODF.

[§] We use the term "deep white matter" to denote all white matter under the white/grey matter boundary. This is in contrast to white matter at the boundary and above where connection terminations occur.

Local streamline methods can be further subdivided into deterministic and probabilistic, depending on whether they perform a deterministic or stochastic estimation. Deterministic methods [63, 81] provide a point estimate of the path of least-hindrance to diffusion between two points. Probabilistic methods [42, 82] estimate a spatial distribution for this path. They estimate the uncertainty around the local fODF peaks (through parametric or non-parametric inference) [42, 82, 91] and account for this uncertainty to obtain the path distribution (peak-based methods). A variant of these approaches use samples from the whole fODF to obtain the distribution (whole-fODF methods, see [92] for an illustration of this difference).

Several studies have evaluated the test-retest reliability of these methods for connectome reconstruction [93-95]. Estimates derived from probabilistic tractography generally show greater connectome reproducibility than deterministic methods, reduce the effect of residual spatial misalignment errors and potentially improve some of the statistical properties of the sampled paths (i.e. normality). At the same time, they can be to the detriment of connectome specificity and accuracy [96]. Probabilistic tractography yields greater spatial dispersion in streamline trajectories, which may lead to more spurious connections (particularly for whole-fODF sampling methods [97]). On the other hand, connectomes derived from deterministic tractography generally comprise fewer connections, but results show substantially greater variation within and across individuals (particularly in data with low angular resolution or low signal-to-noise ratio). It is unclear what proportion of this variation represents genuine anatomical variation between individuals, as opposed to noise due to a poor fitting local fiber orientation model, tractography errors or residual misalignment between the streamlines and regional brain atlas.

The seeding strategy also has an effect on finding the edges of a connectome [98]. Typically, streamlines can be initiated from all white matter and the streamlines intersecting pairs of nodes are mapped to the respective edge [8]. This "brute force" approach was originally suggested to be more sensitive at detecting long white matter bundles [99]. An alternative is to seed from the boundary between white and gray matter [100, 101]. Boundary seeding has been recently shown to provide smaller biases of dMRI estimates when compared to biological ground truths (for instance less gyral bias, better predictions of path length distributions, slightly better sensitivity vs specificity performance) [23, 102].

Limitations and Open problems

Diffusion-to-axon mapping is ill posed
Finding connections is based on a mapping from water diffusion to fiber orientations, which is inevitably required due to the indirect nature of dMRI. Such inference is in general an ill-posed problem [60, 61], but the problem

becomes identifiable using approximations and assumptions. Improving data quality and estimation methods to reduce potential errors arising from these assumptions has therefore been at the heart of dMRI research.

MRI voxels (even at high-resolution) are too large to enable the resolution of axons. Thousands of axons coexist within the volume occupied by an imaging voxel. The measured macroscopic signal is therefore considerably far from the scale of interest. As a result, different ground-truth fiber patterns can lead to very similar signal profiles within a voxel. An example is shown in Figure 2a. Voxel-wise fODF estimation does not have the information to differentiate between these patterns, as they correspond to similar signal profiles. The current approaches rely on approximations and typically assume that patterns with fibre orientation dispersion provide evidence for crossing fibres. Looking for and using discrete local maxima in these fODFs (when in reality there is a fanning or a sharp bending pattern) can lead to false positives and negatives [60]. Efforts have been made to extract more continuous features (other than the maxima) from the fODF and go beyond crossing fibres [66, 103-106]. However, taking advantage of this information in tractography is not straightforward and frameworks that explore such integration are missing.

Another factor that compounds the difficulty in identifying local fiber orientations is the axial symmetry of the diffusion signal. Diffusion in opposing directions will give rise to the same measurement. As a result, voxel-wise fODF estimates are antipodally symmetric as well, even if the ground truth patterns are not. Figures 2b and 2c, show the errors caused by ignoring this asymmetry when tracking diverging and converging bundles.

These inherent limitations make tractography methods very prone to errors. Imposing anatomical constraints [56, 101] and/or tractography filtering [107, 108] offer principled ways to reduce false connections. However, they do not solve the problem of missing connections (false negatives), and caution is needed as filtering can generate spurious between-group differences due to the effective re-distribution of streamlines. These limitations highlight the need for new paradigms. For instance, inferring asymmetric fODFs is possible by considering neighborhoods of voxels rather than individual voxels [109-112]. Augmenting tracking with microstructure [113-116] offers a more robust alternative to orientation-based tracking, as estimated bundles have structural features preserved along their route rather than orientation alone.

Finding terminations is inherently limited

Mapping a connectome demands accurate fiber tracking in deep white matter as well as accurate determination of fiber termination points in grey matter. Identifying fiber termination is inherently difficult with tractography [60]. In fact, tractography cannot terminate propagation in an unsupervised manner and heuristics need to be used to determine endpoints. This makes

termination criteria an important choice and is the reason why anatomically-driven rules can improve reliability of results [100, 101]. For instance, crossing the white/gray matter boundary (WGB) multiple times is likely to yield spurious trajectories and propagation within the cortex may be prone to greater errors due to low anisotropy in grey matter.

Recovering laminar organisation of connectivity is an example where finding terminations with current dMRI technology is impossible. Different layers in the cortex may preferentially connect to different regions [17, 117]. Layer-specific orientation information has been shown with extremely high spatial resolution imaging of ex-vivo tissue [118]. But even if this information was available in-vivo (for instance with some variant of [119]), termination points to different layers would not be estimable using tractography [60], as the algorithms are insensitive to synaptic endpoints. Similar problems exist with subcortical/cerebellar nuclei, within which tractography cannot find synaptic termination locations. A difference, however, is that the inherently higher anisotropy *within* major subcortical structures allows topographical organisation and connection patterns to be probed within their volumes (for instance see [42, 120] or figure S3 in [121]). While in the case of cortex, due to low anisotropy, contrast and the inherent resolution limits, we are mostly sensitive to connectional patterns *along* the cortical sheet (WM/GM boundary) (see "Validation-Indirect Evidence" section for examples).

In the cortex, another obstacle that biases the estimation of termination points is the presence of superficial white matter fibres, such as the U-fibres that run parallel to the WGB [122] (see myelin-stained fibres at a sulcal fundus in Figure 3a). The density of these fibres is higher at the sulcal fundi meaning that dMRI-estimated fibre orientations are parallel to the sulcal surface. It is therefore difficult for tractography to traverse the boundary and escape white matter. This under-representation of tractography streamlines at the sulci compared to gyri was first described in [27] as *gyral bias*. This bias is expected to be more evident for finer parcellation schemes and a large number of nodes, yet it can potentially introduce a confound for coarser parcellations as well, particularly when average curvature and sulcal depth profiles vary considerably across nodes.

Quantifying edges

As described above, tractography can provide an estimate of the trajectories representing fiber bundles. Ideally, a connectome should also include estimates of connection strengths (axonal densities, myelination, diameter). Diffusion MRI cannot provide such direct measures [25, 60], but allows estimation of edge weights that indirectly reflect some of these properties of interest. These range from simple binary values, denoting the presence or absence of an edge, to approximations of biophysical properties

10

of connections, reflecting micro- or macro-structure.

Connection strength is most typically quantified using some function of *streamline counts*, the number of streamlines intersecting a pair of regions. Streamline counts can be enumerated for all pairs of regions to populate the cells of a connectivity matrix [7, 8]. Streamlines that are permitted to propagate within grey matter can intersect more than two distinct regions, in which case they contribute to the streamline count for multiple pairs. Anatomical constraints can be imposed to avoid such scenarios, which either terminate streamlines at the white/gray matter interface or within subcortical volumes [101].

Streamline counts can be symmetrized, normalized or transformed in various ways [85], which aims to reduce the effect of confounds reflecting algorithmic choices and ensure better consistency across subjects. Power transforms, in particular the logarithm, can be applied to the streamline counts before analysis to achieve normality. Normalization by node sizes [8, 123] can be used to account for volume/area variability in the chosen gray-matter parcellation. While it may be that larger brain regions are indeed more strongly connected by virtue of anatomy, a greater number of streamlines is likely to terminate in regions with a larger interface between grey and white matter due to the tractography process [53, 100]. Normalization by row and column sums of the matrix, such as fractional scaling, provide enhanced relative contrast of a particular edge to the rest of the edges that involve any of the two connecting nodes and improves the power to predict tracer-measured connection strengths using tractography-derived weights [23].

Diffusion path probabilities, obtained from probabilistic tractography, reflect normalized conditionals of streamline counts given the orientation model, seeding strategy and termination/counting criteria [74, 82]. As discussed before, due to the stochastic generation of streamlines, probabilistic tracking provides a spatial distribution on the path of least hindrance to diffusion. These path probabilities have been recently shown to correlate with connection strength measured using tracers [23], similar to deterministic streamline counts [124]. However, path probabilities are also confounded by many uninteresting factors (such as path geometry, noise, modeling errors), which make direct interpretations difficult [25, 60].

Alternative metrics that reflect *microstructural* properties along edges can be considered as edge weights. For instance, voxel-specific measures of anisotropy can be averaged over all voxels traversed by a path that is assigned to a particular pair of nodes [125]. The resulting tract-averaged measure thus characterizes the anisotropy of a connectome edge as a whole. Other microstructural measures can be also used [125, 126], such as axonal myelin content measures derived from images of magnetization transfer ratio [127, 128]. Different weighting functions can be employed for the averaging process to give greater weight to different parts of the tract (e.g. using streamline counts/probabilities in each voxel can give greater weight in the

main tract core versus the periphery).

Features that reflect tract *macrostructure* are another possibility for edge quantification. In fact, volume and cross-sectional area of paths intuitively relate more directly to connection strength than their microstructure counterparts. In [129] the tract volume is explicitly used in a model to parameterize connection paths using spatial basis functions. Extensive simulations illustrate the potential to infer volume as a probe of apparent connection strength, but high computational demands currently limit exploration and utility in real data are yet to be shown. In [108], a post-processing filter of streamlines is presented based on a generative model of the data from streamlines (similar in spirit to [107, 130]). The filtered streamline counts are proposed as probes of the cross-sectional area of the WM connection underlying an edge. Even if such an interpretation is based on the strong assumption that relative fODF volume fractions reflect relative axonal densities, the filtering increases the biological relevance of the obtained edge weights [102].

Limitations and open problems

The major limitation for quantifying edges is that none of the above approaches provide an inter-regional measure of the number of connecting axons, which is a desirable measure of connectivity strength in many applications. Tract-averaged microstructural measures may provide an interpretable biophysical property per edge. However, it is questionable how informative such properties are when treating connectomes as networks, which would require some proxy of connectivity. In a recent study no correlation was found between such microstructural measures and axonal strengths measured by tracers [124]. On the other hand, functions of streamline counts can be thought to be more relevant in such a network context [23]. However, factors that reflect data quality, algorithmic choices and inherent limitations bias these measures [60].

Future work should also focus on characterizing the distributional and noise properties of connectivity matrices. Connectivity matrices comprising streamline counts derived from probabilistic tractography are likely to show smoother variations between spatially neighboring node pairs compared to deterministic tractography, as streamline trajectories associated with probabilistic tractography are more spatially dispersed.

Distance bias

Streamline counts between distant regions, interconnected by longer tracts, are often smaller than counts between neighboring regions. Algorithmic limitations contribute to this pattern, for instance longer tracts are more difficult to reconstruct with tractography because streamlines must be propagated for a longer distance and each propagation step provides an opportunity for "wrong turns" [131, 132]. However, connection strengths as

measured by tracers follow an exponential decay with connection length, with the majority of connections being short and strong and the long connections being weak, comprising fewer axons [133, 134]. Tracers of course have their own error sources [17], but the extent to which the algorithmic distance bias of tractography is biologically specific remains to be explored.

Seeding bias

When streamlines are seeded from all of white matter, longer tracts are inevitably sampled more abundantly because they occupy a greater volume than shorter tracts. To compensate for this bias towards long tracts, the streamline count can be normalized by the average length of the streamlines contributing to the count [135]. However, given that many tracts are sheet-like and vary considerably in cross-sectional area and morphology, simple normalization factors such as the streamline length might not adequately correct for the over-sampling of tracts occupying greater volumes. Filtering of streamlines via generative models that ensure higher fidelity with the data [107, 108, 130] is another approach that seems to be more beneficial in this context. Initiating streamlines from the WM/GM boundary interface is an alternative that overcomes this limitation and can potentially provide more realistic path length distribution [23, 100, 102], but this seeding approach has difficulty in tracing out long fiber bundles.

Gyral bias

As described in the previous section, the existence of superficial tangential white matter can lead to under-representation of tractography streamlines at the sulci compared to gyri [122], the so-called gyral bias [27]. The bias is further magnified by algorithmic limitations in tractography; sharp turns (which are needed to capture axons that can bend at quasi-right angles [15]) are less preferred than linear trajectories and that will lead most of the times to the gyral crowns.

The gyral bias is biologically relevant. The preferential termination of tractography streamlines at gyral crowns agrees with neuro-anatomical expectations. It is the magnitude of the difference for preference towards gyral crowns compared to sulcal fundi that is unrealistic [27]. Indeed, let's assume that the number of axons crossing the WGB is constant per unit cortical volume (i.e. there is no bias). Cortical folding however induces geometrical differences in different parts of the cortex. Cortex tends to be thickest along gyral crowns and thinnest in sulcal fundi [136] (Figure 3b), and larger cortical volume corresponds to a unit surface area of the WGB at the crown compared to the fundus. Therefore, even if the number of axons crossing the WGB boundary is roughly the same along it, the density of axons crossing at the gyral crowns will be larger compared to the ones crossing at the sulcal fundi. Van Essen et al used cortical thickness measures to compute

this expected bias (Figure 3c) and found that it is 4-5 times less than the one predicted by tractography [27].

New paradigms are needed to address these limitations when tracking close to the WGB. Some very recent studies have taken preliminary steps in this direction. In [137] the relationship of fibre orientations with cortical features is explored using post-mortem high-resolution histology and used to inform generative models for in-vivo diffusion MRI. In [138] a strong prior is imposed on the fibre orientations within the cortical ribbon and flow preservation constraints are used to successfully track into/out of various locations along the WGB. Approaches for neighbourhood-wise tracking, as the ones used before for deep white matter [110], may also be beneficial for better estimating the transition between white and gray matter.

Counting using surfaces or volumes?

Boundaries, such as the WGB, can be represented either as volumes or as surface meshes. Surface representations offer a more compact and accurate description of the boundaries at a given resolution [139]. This can have an effect on the tractography results and their interpretation. For instance, an intermediate-resolution, voxel-based representation of the WGB cannot necessarily follow the highly convoluted boundary (Figure 3d) and can mask the gyral bias. As shown in the inset of Figure 3d, the streamlines are frequently unable to reach a voxel representing the gyral crown, without first traversing a voxel that represents the sulcal fundus. Depending on the width of a gyrus and on how tractography boundary conditions are imposed, this can artificially increase the visitation frequency to certain sulcal regions (blue asterisks in Figure 3d). However, these frequencies and their spatial pattern may purely reflect resolution-induced limitations of the voxel-wise representation. Using surface meshes, such as GIFTI files [139], should be more robust to these problems, but the exact differences between results obtained from the two representations remain to be explored.

Summary

The reconstruction and mapping of connectome edges is confounded by many limitations and open problems remain to be solved. Reproducible, sensitive, specific and biologically interpretable measures of white matter connections are difficult to obtain with diffusion MRI. Despite these limitations, diffusion MRI enables reconstruction of connectomes, which display biological properties that are consistent with brain networks mapped with alternative modalities. Recent studies explore this directly [23, 102, 124], while a plethora of studies provide indirect evidence in favor of consistency between modalities. We review this evidence in detail in the *Validation* section of the paper.

Impact of data quality

So far we have discussed the impact of algorithmic and methodological choices on building connectomes. Another important aspect that affects estimation of dMRI-derived quantities in general (and therefore connectomes) is data quality. Given the inherent limitations of diffusion MRI, better data can help if developments allow: a) improvements in diffusion-to-axon mapping and b) reduction in partial volume. Signal-to-noise-ratio (SNR), spatial resolution, angular resolution and angular contrast are some of the data features that can directly influence these factors [28]. Even if some limitations cannot be directly overcome with better data (see [122] and some of the conceptual problems described in the previous sections), significant improvements in tracking white matter have been shown.

More specifically, better SNR and/or angular resolution improve precision and accuracy of the mapping from diffusion signal to fiber orientation estimates [140]. Improved angular contrast allows higher sensitivity in detecting within-voxel complex fiber patterns [69, 73, 76], which further allows more accurate tractography [74]. Multiple angular contrasts (i.e. b values) give better estimation of partial volume and differentiation of diffusion compartments and further augment accuracy of orientation estimates [141, 142].

Increased spatial resolution reduces partial volume and allows imaging of exquisite details of white matter organisation [143-145]. For instance, very high-resolution dMRI allowed the mapping of axonal and dendritic networks in the hippocampus, whose accuracy was confirmed with tracers. High spatial resolution is also beneficial for distinguishing correct tract termination points [146]. Increasing the resolution by using high field strength improved the estimation of the fibre spreading pattern to the cortex and reduced gyral bias [147]. In another recent study, improving on all the data quality aspects of dMRI data increased agreement of connectomes estimated in humans using three different modalities [148].

In Figure 4, we illustrate a simple example of how changing spatial and angular resolution of the data affects tractography. In that particular case, the increased spatial resolution is beneficial in differentiating thin projections from the hand area of the motor cortex. Apart from better resolving partial volume, higher spatial resolution is expected to increase the estimation accuracy of relatively short paths, which comprise the majority of brain connections [19, 133]. We need to point out, however, that increasing spatial resolution at the expense of Contrast to Noise Ratio (CNR) or angular resolution can actually lead to suboptimal performance [146, 149], particularly in tracking major bundles.

Deciding on the acquisition protocol and getting the balance of these features right is governed by a series of trade-offs (for instance SNR competing against spatial resolution or angular contrast). As shown in Figure

4, it may not be optimal if a feature is improved at the expense of others. Recent frameworks attempt to resolve these trade-offs by fusing complementary datasets (e.g. data with high spatial & low angular resolution with data with low spatial and high angular resolution) [147, 150]. Another group of post-processing methods boost certain features to improve estimation. These include denoising approaches for improving SNR [151, 152] and up-sampling or super-resolution methods for improving spatial/angular resolution [153-155]. Nevertheless, we can expect recent technological advances to provide better operating points for all these competing features and improve overall data quality. Hardware developments in modern scanners [156], such as higher gradient strengths, can translate to improvements in SNR and contrast of routine scans. While higher field strengths might pose difficulties to dMRI acquisitions due to the shorter T_2 relaxation times at high field [156], they can be used to achieve very high spatial resolution [143, 157].

Sequence developments should accompany these hardware advances. For instance, simultaneous multislice or multiband acquisitions [158, 159], allow 3-5-fold acceleration of dMRI scan time, changing the perception of the data quality that can be achieved in realistic time frames. Faster scan times translate to higher spatial and/or angular resolution and/or SNR per unit time. Diffusion-sensitization using double-pulsed field gradients (see [160] for a review) or generalized trajectory imaging [161] open new possibilities in probing restricted compartments and microscopic features with the potential to improve the accuracy of mapping from diffusion measurements to tissue structure.

Better data enable improved modeling and analysis [60]. In fact, new tools are required to take full advantage of the new information in certain applications. An example is increasing spatial resolution in the presence of inevitable subject motion and eddy currents. The higher the aimed resolution, the higher the need is for accuracy in distortion correction tools. New frameworks in this area [162, 163] have been shown to limit alignment errors between dMRI volumes to less than a quarter of the voxel size [164] and improve distortion correction [165], therefore preserving the benefits of high resolution acquisitions after preprocessing.

Validation - Comparison with other modalities

We have highlighted a series of limitations for mapping the connectome using diffusion MRI. It is therefore important to quantify the effect of these limitations on the ability to accurately map connectomes. It is also important to explore the utility and biological consistency of current connectome mappings given the limitations of dMRI and tractography. More and more frameworks are developed towards this aim (e.g. [78, 97, 166-168]).

In the following sections we review studies that specifically compare tractography-induced estimates with estimates from other modalities; either directly for the purpose of validation or indirectly for the purpose of multi-modal integration. The comparisons show differences (and limitations as highlighted in the previous sections), but also provide evidence of agreement and predictive power in various different contexts that are greater than expected due to chance.

Direct evidence

There have been efforts to directly validate parts and aspects of the tractography-estimated connectome with a different invasive modality, such as chemical tracers, primarily in animals. Tracers have their own limitations and biases [17]. For instance, identifying correspondence between injection sites and a particular brain area is not straightforward. Axons that traverse the injection site can result in the reconstruction of spurious connections because these axons can absorb the tracer even though they make no synaptic contacts with the injection site. Absolute quantification of connection strength is also difficult, as anterograde and retrograde tracers depict different features of connectivity. However, tracers are very precise in spatial localisation and have a considerably lower false positive rate than tractography. Thus, even if not perfect ground truths, they are much closer to the ground truth than in-vivo dMRI.

Validation efforts have focused on the existence of edges and/or on their relative strength (i.e. treating the connectome as a binary or weighted matrix, respectively). The main conclusions that can be drawn are: 1) Tractography predictions are above chance, however features with poor agreement exist. 2) There is a trade-off between sensitivity and specificity. Tractography methods that tend to be more sensitive in finding connections are also less specific. 3) Cortico-subcortical, short-range intra-hemispheric and homotopic inter-hemispheric connections are more reliably estimated. 4) Weights estimated by tractography can be fair but far from perfect predictors of the underlying connection strength. 5) Parcellated connectomes, i.e. estimated with nodes corresponding to mid-scale regions, are more accurate than denser ones that attempt to depict fine, within region, details. In the following paragraphs we review the relevant studies and findings in more detail.

Identifying the existence of connections

The first validation studies investigated how well tractography can identify large bundles and follow them through white matter. Qualitative comparisons have shown good agreement against histological tracing in the monkey brain [169] or against dissected human samples [170, 171]. Newer dissection methods [172] allow preservation of the cortex and of the superficial white matter and have shown examples of the ability of tractography to follow the true route of connections up to their terminations [173, 174]. However, semi-quantitative comparisons have also highlighted false positive connections that are estimated [175, 176].

The sensitivity (finding true connections) and specificity (avoiding false connections) of tractography in detecting connectome edges has been more systematically explored in comparison to chemical tract tracing in the monkey [23, 90, 177, 178], mouse [55, 56] or porcine brain [179]. Areas under the curve in receiver-operating characteristic (ROC) plots have been reported in the range of 0.7 to 0.8 suggesting a fair estimation accuracy in identifying connections and/or their routes (Figure 5a). At the same time, all studies illustrate the strong dependence of the results to the particular tractography settings and models. Probabilistic tractography is less sensitive than deterministic to anisotropy and curvature thresholds or the tissue composition of the seed [177, 178]. It also tends to be more sensitive, but less specific than deterministic methods and more susceptible to false positives [97, 177, 179]. In general, an increase in sensitivity for all methods comes at the expense of a decrease in specificity and therefore a need for an optimised set of parameters is important. Also, tractography performs much better when exploring connections between relatively large cortical nodes rather than fine details within regions.

Comparisons of dMRI-estimated paths with tracers also reveal benefits of considering fibre crossings in tracking (in some cases larger benefits are shown [179] than in others [177]). Adding prior knowledge to guide connectome mapping is also beneficial [56]. In [180], organisational principles of cortical projections identified with tracers were found and generalised to post-mortem macaque MRI data using informed tractography protocols that included a-priori specified waypoint and exclusion masks. These were then used to search for and identify similar principles in humans. In [181], subcortical connectivity signatures were obtained and revealed a series of networks between basal ganglia sub-nuclei and the cortex. Some of these networks, in particular cortico-striatal circuits, were directly validated against previous tracing studies in monkeys.

Tractography-estimated weights

An even more challenging task than localising connections is extracting relative weights for the connectome edges. The recent development of comprehensive and weighted brain mappings by collating a

18

plethora of tracing experiments [19, 20] has permitted the direct comparison with tractography-derived connectomes. Out of these studies, we can extract some general features of the connectivity weights as measured by tracers: 1) There is a wide range of connectivity strengths than spans five orders of magnitude. 2) An exponential reduction of connectivity strength occurs with path length [133, 134]. 3) There is a prevalence of local connections. Short connections are significantly more and significantly stronger than long connections.

In one of the most recent comparisons, the authors evaluated the accuracy of dMRI connectomes in predicting generic features extracted from human brain dissections [102]. The connectome edges and weights correctly replicated the relative percentage of long inter-hemispheric and intra-hemispheric connections and the inverse relationship between connection strength and length.

Non-human primate studies allow more detailed comparisons due to the plethora of available ground-truth. In [23] the connectome edges and weights obtained via macaque tractography and macaque tracers were compared. Tractography could recover four out of the five orders of magnitude in the range of connection strengths. The performance was far from perfect, yet better than chance, even for the weakest longest paths (Figure 5a). Strong and short connections were better characterised by tractography, as the performance worsened with smaller connection weights. Overall a correlation of ~0.55[**] was reported between edge weights in tracer and tractography and the path length dependence contributed significantly to this correlation. Interestingly, however, after regressing out path lengths, there was still a significant correlation (but smaller ~0.25) between the two measures, showing that it is not only the path length dependence that drives the relationship. Similar trends were reported in [124] (though with smaller overall correlations ~0.35, but a different definition of connectome weights).

The dependence of these correlations to the node size was explored in [55, 56] for the mouse brain. Connection weights between mid-level sized regions were more reliable (correlation up to 0.77 in [56]) compared to considering small nodes (correlation dropped to 0.45). Similarly for the monkey brain [57]. As discussed in the previous sections, certain limitations reduce the reliability of tractography at finer scales. Despite the errors, all the validation studies provide evidence that dMRI-induced connectomes contain relevant information and predictive power. Interpretation might not always be straightforward, but a large number of applications show that this information can be useful. We review some of these applications in the following section.

[**] To put these correlation values into perspective, comparisons between histology and MRI-derived values of a much more straightforward feature, such as cortical thickness, give correlations in the order of 0.6-0.7 [182, 183], reflecting the inter-modality variability and difficulty of direct comparisons.

Indirect evidence

The idea of connectivity fingerprinting using tractography weights (Figure 5b) [4] has been applied to identify boundaries of functionally distinct regions (see [45, 184] for reviews). In one of the earliest studies [43], a dense weighted matrix mapping connections from the medial frontal cortex to the rest of the brain was obtained using tractography. This matrix was used to identify the boundary between the anterior and posterior part of the supplementary motor area. These are functionally distinct areas both in motor and cognitive domains and the boundary, identified as a sharp change in the tractography profiles, agreed well with the one obtained from functional MRI localizer tasks. Since then, similar results in predicting functional boundaries using dMRI and agreement with functional MRI have been shown for various cortical [41, 44, 185-191] and subcortical areas [42, 192-194] (see Figure 5c). Agreements have been also illustrated with other non-MRI functional measurements, including PET [120] and direct electrophysiological recordings [195], as well as cytoarchitectonic delineations [196, 197].

Tractography "signatures" can be reproducible and robust across subjects to a degree that allows predictions for the efficacy of targets in functional neurosurgery [198, 199]. In deep brain stimulation, neurosurgeons search for the most efficient stimulation target via trial and error. In [200] the authors identified in that classical way the thalamic location, which when targeted for stimulation allowed the most efficient alleviation of tremor symptoms. They then estimated using previously acquired dMRI the connectivity fingerprint of that region. New patients were scanned prior to surgery and the thalamic region best matching this fingerprint was identified and used as initial target for stimulation. They found that in these new patients the tractography-informed target was indeed very close to the most efficacious location, allowing better surgical planning.

The functional relevance of structural connectomes has been further illustrated by studies that use structure to constrain or predict function (Figure 5d). Models of functional networks built on a structural backbone have increased explanatory power and identifiability compared to models that lack such structure [201, 202]. Structural connectivity networks alone have been used to predict the existence, strength and spatial features of functional connections as assessed by fMRI at rest [203]. During a task, the functional activation maps have been predicted solely by the connection pattern of the activated region [5]. More specifically, the authors in [5] learnt a model in a group of subjects between the tractography-estimated connectome of the fusiform gyrus and the functional activity recorded via fMRI during a face selection task. They then applied that model to the connectome of new subjects and they predicted their task activation. This predicted activation was found to be very similar to the individually measured activation by subsequent fMRI. A subsequent study used a similar mapping approach and predicted the functional organisation in young children after they learned how to read, using

the structural connection patterns they had developed prior to acquiring this skill (i.e. a few years earlier in their development) [204]. Such structure-function relationships can be observed even at a higher-level, with structural connections predicting behavior and decision-making processes [205-207].

Mapping gray-matter connection patterns offers the unique ability to perform comparative anatomy (see [208] for a review). This allows the identification of "homologue" areas across species (areas that share similar "connectivity contrast") and the translation of the vast literature of animal studies to humans [209-212]; but also translation from humans to other primates to study evolution [213-216]. Such studies provide evidence of agreement of the structural estimates with a large range of independent sources of information.

Network analysis

Connectivity fingerprinting approaches discussed in the previous section (Figure 5b,c) mostly reflect hypothesis-driven analyses, where a subset of the connectome is considered and relative connection patterns associated with certain nodes are examined. An alternative approach considers network properties, either in a data-driven manner or with respect to hypothesis-driven regions. Complex networks have been studied in mathematics for centuries, where they are known as graphs and are fully defined by their nodes and edges (Figure 1 and Figure 6). In this section, we consider how graph theory and network science can be used to understand the global organization of the connectome.

The edges of a graph are either directed or undirected. Edges inferred from tractography are invariably undirected because the direction of diffusion cannot be resolved with diffusion MRI (in contrast to tract tracing methods that can distinguish between afferent and efferent fibers). Furthermore, the edges of the graph can be either weighted or binary, as previously discussed.

Adjusting density and weights

Thresholding methods applied to brain graphs with weighted edges reduce the density of connections in a graph and aim to eliminate spurious edges, thus improving specificity. Thresholding can be further applied to binarize graphs [217, 218] and simplify the interpretability of certain analyses by emphasizing network properties that may be obscured by large variations in edge weights. On the other hand, thresholding may disregard useful information (see previous section and representative examples in [5, 43, 205]). Therefore, the applicability of such approaches depends on the particular question of interest.

The simplest thresholding method, called *weight-based thresholding,* involves eliminating any edges with a weight that is below a given global threshold. To yield a binary graph, the weights associated with the remaining edges are disregarded, leaving only information about whether edges are absent (0 in connectivity matrix) or present (1 in connectivity matrix). Weight-based thresholding introduces the confound of graph density to comparisons between groups of individuals. Graph density[††] —the proportion of all node pairs that are directly interconnected by an edge— fundamentally influences the properties of a graph [218]. Applying the same global threshold to different brain graphs does not necessarily ensure that the resulting thresholded graphs have the same density. Therefore, when complex properties of thresholded brain graphs are found to differ between individuals,

---

[††] The term "connection density" is found in the relevant literature. We use "graph density" here to avoid confusion with connection axonal density that we refer to in other sections of the paper.

it is unclear whether these differences are trivially owing to differences in graph density.

Density-based thresholding [218] overcomes this confound. A unique threshold is determined for each individual to ensure a fixed graph density for all individuals. The disadvantage of this approach is that the number of spurious connections may differ between individuals because different absolute thresholds are used, which introduces a new confound.

The differences between thresholding methods are evident when comparing brain graphs between different groups (e.g. patients and healthy controls) [217]. For instance, many white matter connections in patients with schizophrenia comprise significantly fewer streamlines when compared to healthy individuals [219]. Therefore, density-based thresholding is likely to result in brain graphs that comprise more spurious connections in patients compared to controls [220]. This may explain the subtle randomization of network organization reported in patients with schizophrenia [219, 221]. In particular, density-based thresholding may force the inclusion of spurious edges into the patient brain graphs, leading to randomization. On the other hand, if weight-based thresholding is used, it is important to recognize that potential differences in complex network properties may simply reflect a lower overall number of connections in one group. Ultimately, the distinction between these two thresholding methods boils down to whether differences in complex network properties should be divorced from differences in graph density.

A variety of alternative thresholding methods have been developed to preserve or emphasize specific features of brain graphs. Fragmentation of a graph into disconnected islands of nodes is undesirable and anatomically unrealistic. To avoid fragmentation, a *minimum spanning tree* can be formed based on the edges with the highest weights [222]. By definition, this yields a connected graph in which paths can be found between all node pairs. Further edges can then be progressively added to the minimum spanning tree until a desired graph density is achieved. Local thresholding methods attempt to preserve graph structures that span multiple scales of edge weights. Whereas global thresholding is invariably based on a single threshold, local thresholding methods such as the disparity filter [223] seek to calculate distinct thresholds for each node and its associated connections. Finally, thresholding can be performed to preserve edges that are consistently found between a group of individuals [224]. Such consistency-based thresholding can however eliminate connections that genuinely vary between individuals.

While thresholding is not an essential prerequisite to brain graph analysis (see for instance the connectivity fingerprinting examples described in the Validation section and in Figure 5), it is often performed to: i) improve the interpretation of topological descriptors, ii) ease computational and storage burden; iii) control for the effect of between-group differences in graph density when performing between-group comparisons of network

properties; and, iv) minimize the number of spurious (false positive) connections. Including spurious connections (false positives) is substantially more detrimental to the topological analysis of brain graphs than failing to detect genuine connections (false negatives), and thus thresholding is considered a crucial step to maximize the specificity of brain graphs [96]. The choice of thresholding method (if any) should be guided by the requirements of subsequent analyses. For example, thresholding methods that yield binary graphs are inappropriate if the goal is to test for between-group differences in the weights associated with each edge.

Network properties of brain graphs

Many intriguing properties of brain graphs have been discovered during the last decade. These properties are not unique to the human brain and are often found universally across many species and imaging scales. Brain graphs are *small-world* networks that are *modular* in structure [225]. Modular small-world networks are characterized by communities of nodes that are densely interconnected among themselves, predominantly with relatively short connections, while also sparsely connected to other communities by a small number of long-distance connections (Figure 6a). These densely interconnected communities (modules) are hypothesized to facilitate network segregation and specialized information processing. The longer connections interconnecting these modules facilitate network integration and distributed information processing. Modules in brain graphs tend to be spatially localized and comprise cortical regions that perform specialized functions, such as visual, auditory or motor processing tasks.

Brain graphs also comprise a densely interconnected core of *hub nodes* that form a *rich club* [226]. Hub nodes make connections with many other nodes and serve as focal points for the divergence and convergence of neural information. Hubs are defined as nodes with large degrees, where the *degree* of a node is simply the total number of other nodes to which it is directly connected [227]. The nodes of brain graphs differ very substantially in degree. Indeed, the distribution of nodal degrees in most brain graphs can be described by a truncated power law (scale-free distribution), which implies the existence of a small number of highly-connected hub nodes. For a hub node to form part of the rich club, it must also be densely connected with other rich-club nodes. A rich club in general comprises nodes (hubs or non-hubs) that are both densely connected among themselves as well as with other nodes. Non-hub nodes of the club are called peripheral or local nodes. Rich clubs are synonymous with many kinds of natural and engineered networks. For example, major air transportation hubs are interconnected to an extent that is significantly greater than expected in random networks with the same nodal degree distribution. While the hub nodes comprising a rich club are usually distributed across different modules, they are also densely interconnected by long-range connections. This suggests that the rich club is a network core

that plays a crucial role in integrating and coordinating the activities of specialized modules. Typical hub nodes comprising the rich club of brain graphs include the caudate, thalamus, precuneus, superior frontal gyrus and middle cingulate gyrus (Figure 6b).

Another property of brain graphs is *network economy* [228]. Brain graphs are spatially embedded networks in which each node is associated with a coordinate in Euclidean space and each edge has a physical length [135]. Long connections are considered costly to nervous systems in the sense that they occupy more physical space and consume more metabolic resources [229]. A small number of long-distance connections is however crucial to ensure information can be efficiently integrated between different modules. Spatially embedded networks that comprise only short connections are not very costly in terms of their energy and space requirements, but they are also not very efficient integrators of information. Indeed, spatially embedded networks comprising only short connections are lattice-like networks in which distant pairs of nodes must traverse many connections to communicate. The number of connections that need to be traversed, known as the *path length*, can be drastically reduced with the addition of a small number of long-distance connections [230]. Network economy refers to this tradeoff between the cost of a network's topology and the efficiency with which that network can integrate information (Figure 6c). In practice, efficiency is quantified as the inverse of the path length between all node pairs [231], while cost is quantified as the sum of the physical length of all connections. Numerous studies indicate that nervous systems have evolved to negotiate a compromise between network efficiency and network cost [232].

Comparing network properties between groups
Comparing the network properties of brain graphs between groups of individuals can reveal new insights into brain network organization in health and disease (see [10] for an extensive review). Statistical inference can be performed on the connectome at many different scales. The simplest data-driven approach is to independently test the weights associated with each edge for a between-group difference or a statistical association with some measure of cognitive performance. Network-specific methods can be used to identify between-group differences given the network structure and correct for multiple comparisons. The network-based statistic [233, 234] is an example of one such non-parametric approach that identifies interconnected subnetworks for which the null hypothesis (of no differences between groups or no associations with chosen score) can be rejected. Given that brain pathology seldom impacts a single connection in isolation [235], these mass univariate approaches aim to identify multiple network elements that significantly differ in connectivity strength between groups. In many brain diseases, white matter connections provide conduits that promote the spread and spatial propagation

of a pathological mechanism [236, 237], and thus it is not surprising that disease-related connectivity effects often form interconnected subnetworks (Figure 6d).

Another approach to statistical inference is the testing of between-group differences in global summary measures of network organization, such as measures of network efficiency [228], small-worldness [238] and modularity [239]. Global testing is simple but lacks specificity, in that insight cannot be gained into whether effects are distributed throughout the brain, or confined to a specific set of nodes or edges. Finally, multivariate statistical inference is growing in popularity and can play an important role in the future as datasets continue to increase in size and complexity. Multivariate approaches seek to learn complex patterns among multiple elements of a brain graph and utilize these patterns for inferential classification and prediction. Support vector machines [240], partial least squares [241] and canonical correlation analysis [242] have been successfully applied to connectomic data.

Interpreting clinical differences in brain graphs can be challenging. These can be further complicated due to the complex patterns of epiphenomena and adaptive responses, as well as the progressive nature of connectivity deficits in many brain diseases. In general, analysis of brain graphs in clinical populations requires care in the choice of network measures analyzed—testing for between-group differences in a large set of arbitrarily chosen properties of a brain graph is unlikely to be fruitful. Ascribing biological meaning to some network measures is also challenging and based on many assumptions. For example, measures of path length tacitly assume neural information is transmitted via the shortest paths in a brain graph [228, 229], but this remains to be established and other models of transmission based on diffusion processes and greedy navigation may be considered more plausible [243].

Summary

Using diffusion MRI to map macro-connectomes in vivo has shown promise in exploring brain organisation and advancing our knowledge of brain connection patterns and network properties that are difficult to elucidate with alternative techniques.

However, mapping connectomes with diffusion MRI remains challenging and caution is needed to ensure that connectomic analyses do not demand or assume fiber reconstruction accuracies that stretch beyond inherent limitations of macroscale imaging modalities. It is important for investigators to be aware of these existing limitations that affect the applicability, accuracy and interpretation of connectome reconstructions. Open problems in the various stages of building connectomes set new interesting and challenging questions. They provide new opportunities for acquisition and methodological developments, which are necessary to progress the field. Validation studies based on microscopy, tracers and histology are also needed. Such comparisons can assist with identifying the major challenges and modes of failure in a systematic way and motivate new developments.

Multimodal imaging and analysis may overcome some of the limitations of dMRI. Apart from using dMRI, brain networks can be also estimated using anatomical [244], resting-state functional [245] and task-based functional MRI [246], while temporal dynamics can be estimated using MEG [247] and EEG [248]. Since all these approaches are indirect, each is accompanied with its own assumptions, limitations and independent sources of errors [17]. Therefore, having multiple windows to the true physical connectivity can filter out inaccuracies inherent to particular modalities and provide stronger support for the reliability of the findings [148]. This cross-modal paradigm has been used by large initiatives, for instance the Human Connectome Project [121, 249], and has proved beneficial in demanding problems [39].

Currently, estimated parcellated connectomes with nodes corresponding to relatively large regions are more robust and reproducible, but they are also more likely to overlook detailed patterns of connectivity. Dense parcellations have proven useful when parts of the connectome are considered in a controlled, hypothesis-driven analysis. However, they can potentially introduce difficulties in estimation when the connectome as a whole is to be used in an exploratory fashion. In the future, we can expect that solving some of the open problems will increase the accuracy of the different representations.
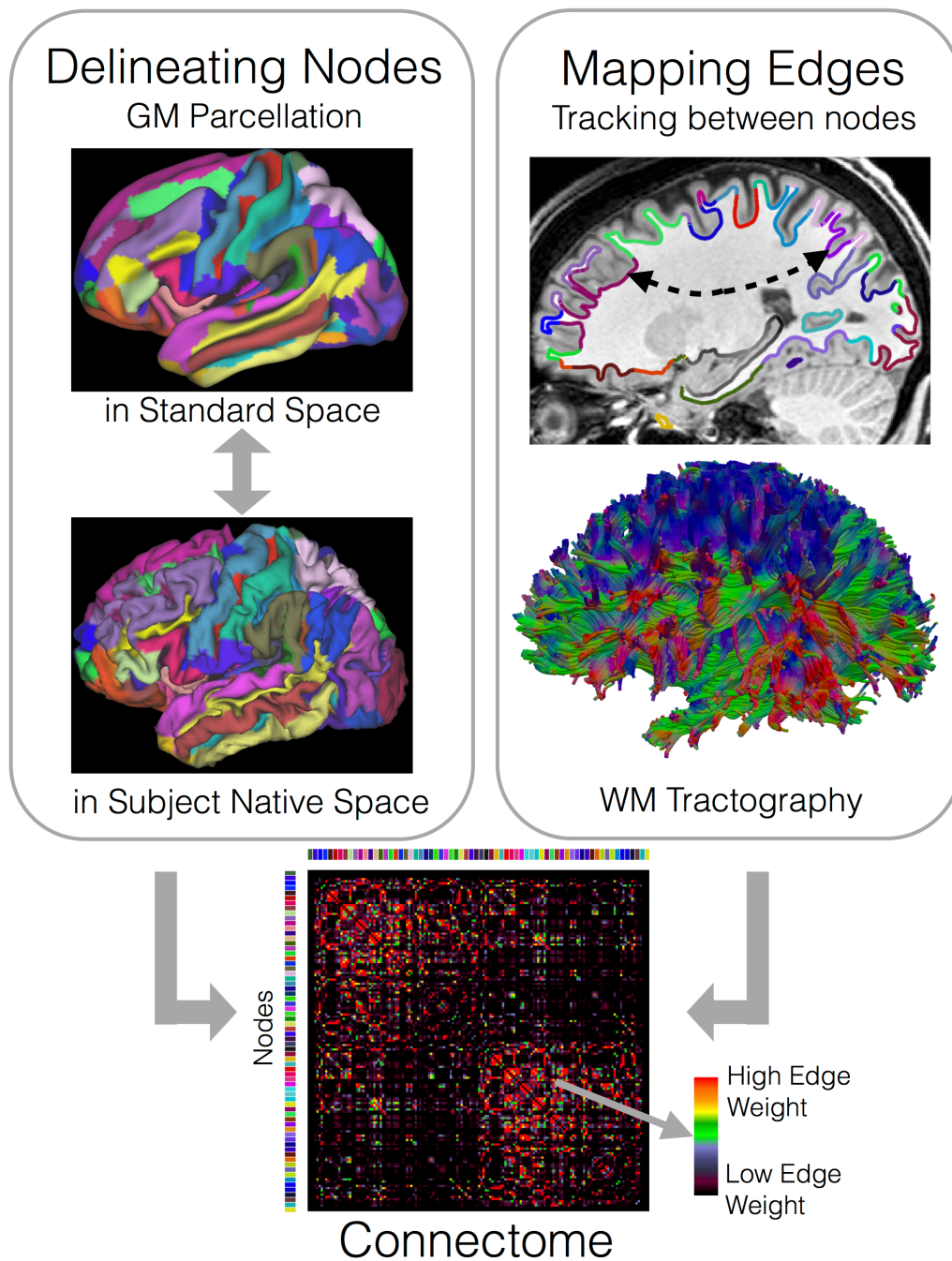
Figure 1. Generating a macroscale connectome involves estimating its nodes and edges. The nodes are typically gray matter (GM) regions (cortical and subcortical) defined either geometrically, functionally or cyto/myelo-architectonically. The edges represent connection pathways between the nodes. Diffusion MRI and tractography can probe these white matter (WM) connections and estimate relative weights.
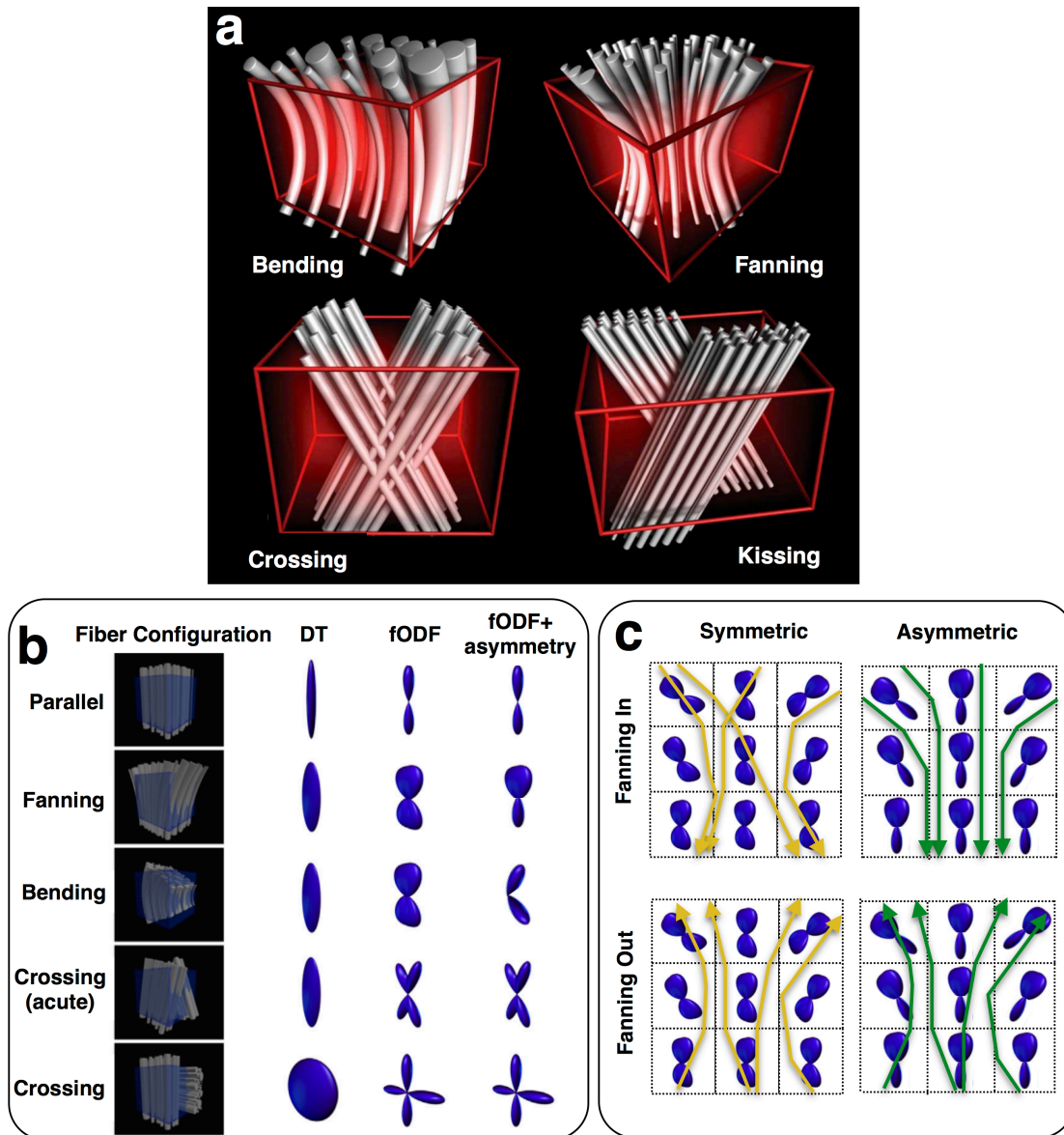
Figure 2. a) Examples of complex fibre patterns that can result to very similar within-voxel diffusion MRI signals. Reproduced with permission from [61]. b) The estimated diffusion tensor (DT) and fibre orientation density function (fODF) are shown for different patterns. The last column shows an asymmetric fODF, which cannot be estimated in practice given that the voxel-wise dMRI signal is inherently antipodally symmetric. Modified with permission from [62]. c) Hypothetical example showing what the effect of asymmetric fODFs in tracking fanning geometries would be. The asymmetry in voxel-wise estimates provides asymmetry in propagation, with the aim of reducing false positives in the case of tracking converging (fanning in) geometries. Recreated from [60].
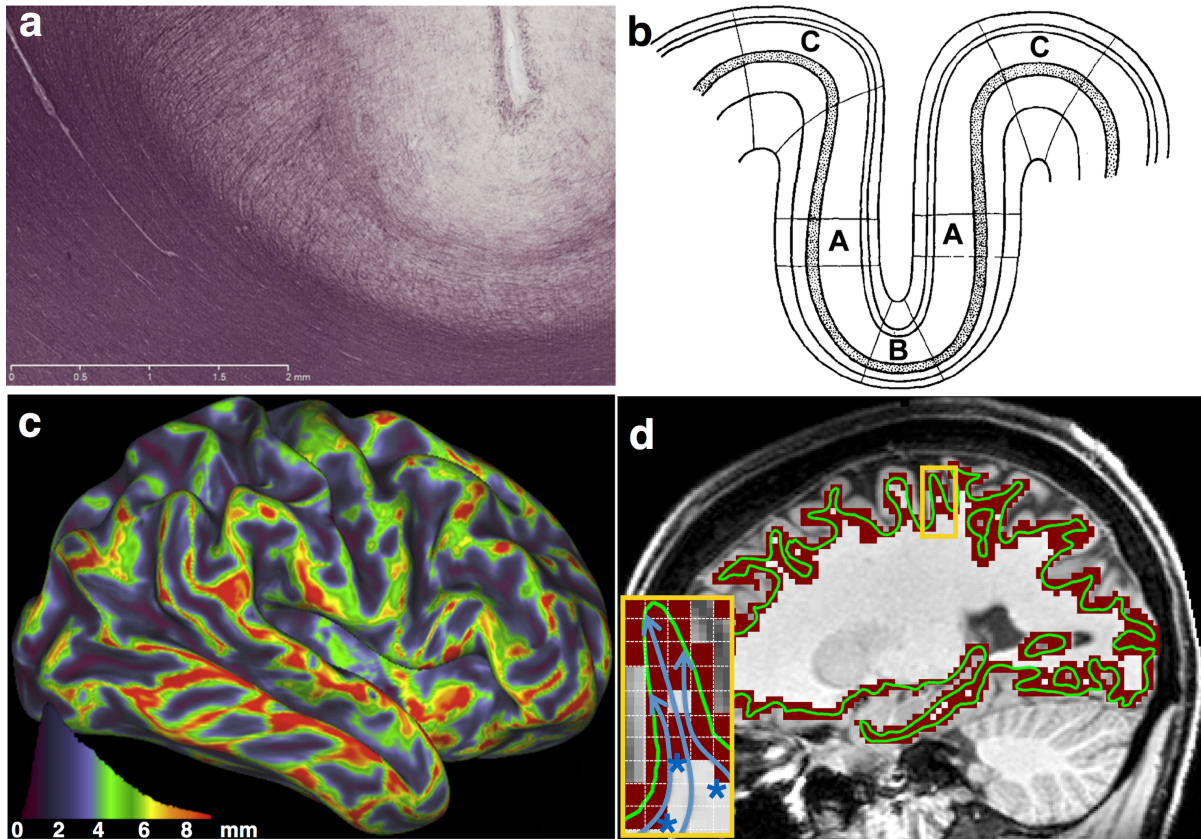
Figure 3. a) A myelin-stained slice showing fiber patterns in the cingulate sulcus of a 18-month-old macaque. The major fiber orientations run parallel to the WM/GM boundary. b) Folding-related effects on radial axes and cortical thickness. The cortex is thinnest at the sulcal fundi (region B) and thickest at the gyral crowns (region C). c) Expected gyral bias based on estimated surfaces and cortical thickness. The cortical volume (mm^3) per mm^2 surface area of the WM/GM boundary surface is displayed on an inflated human brain (right hemisphere). Panels (a), (b), (c) are adapted with permission from [27]. d) Defining boundaries using surfaces vs volumes. The white-gray matter boundary is shown as a surface (green outline) comprising vertices that are 2mm apart. The same boundary has been projected to a volume (dark red region) comprising voxels that are 2mm apart. The projection was performed using for each vertex of the 3D surface the nearest voxel. Both boundaries are superimposed on a high-resolution T1w image (sagittal view). The inset (yellow outline) shows a magnified view of a gyrus, as it is described by the two methods. The volumetric description lacks specificity and precludes differentiation of termination points of incoming pathways (blue curves) at different locations of the boundary. For instance, locations at the sulcal fundi (blue asterisks) can be perceived as termination points of the incoming streamlines, even if these are directed towards the gyral walls and crown.
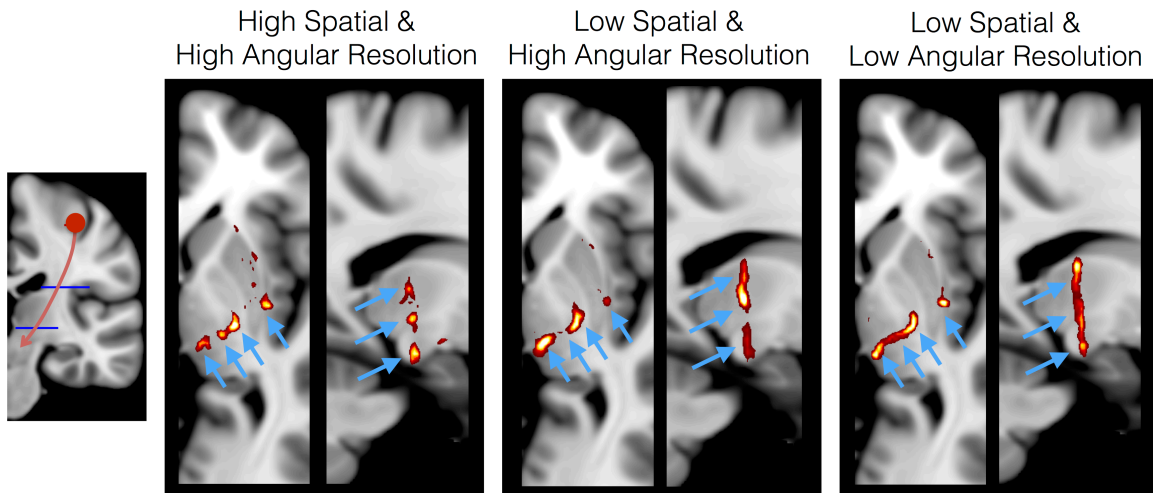
Figure 4. Tractography results from the hand area of the motor cortex for different spatial and angular resolutions. The same subject was scanned at two different spatial resolutions: $(1.35mm)^3$ and $(2.5mm)^3$ using a Siemens Prisma 3T. The diffusion sensitisation followed a HCP-like dMRI protocol (with 3 b values=1000, 2000, 3000 s/mm^2 and 90 directions per b value) [145] and identical preprocessing was applied to both datasets [250]. The former dataset represented a high spatial and angular resolution scan, and the latter dataset a low spatial and high angular resolution counterpart. A subset of the 2.5mm dataset with 60 uniform directions for b=2000 s/mm^2 was used to represent low spatial and low angular resolution. Up to 3 fibre orientations were estimated in each voxel of each dataset using the generalised ball & stick model [141]. A tractography protocol defined in MNI space was then used (left panel), including a seed region at the hand area of the motor cortex (red) and two axial waypoint masks at the internal capsule (blue). The modes of the path distributions obtained using probabilistic tractography are shown for each case (results thresholded at path probabilities of 0.5%) in axial and sagittal views. The four arrows correspond from medial to lateral to: cortico-thalamic, cortico-bulbar, cortico-spinal and cortico-striatal projections.
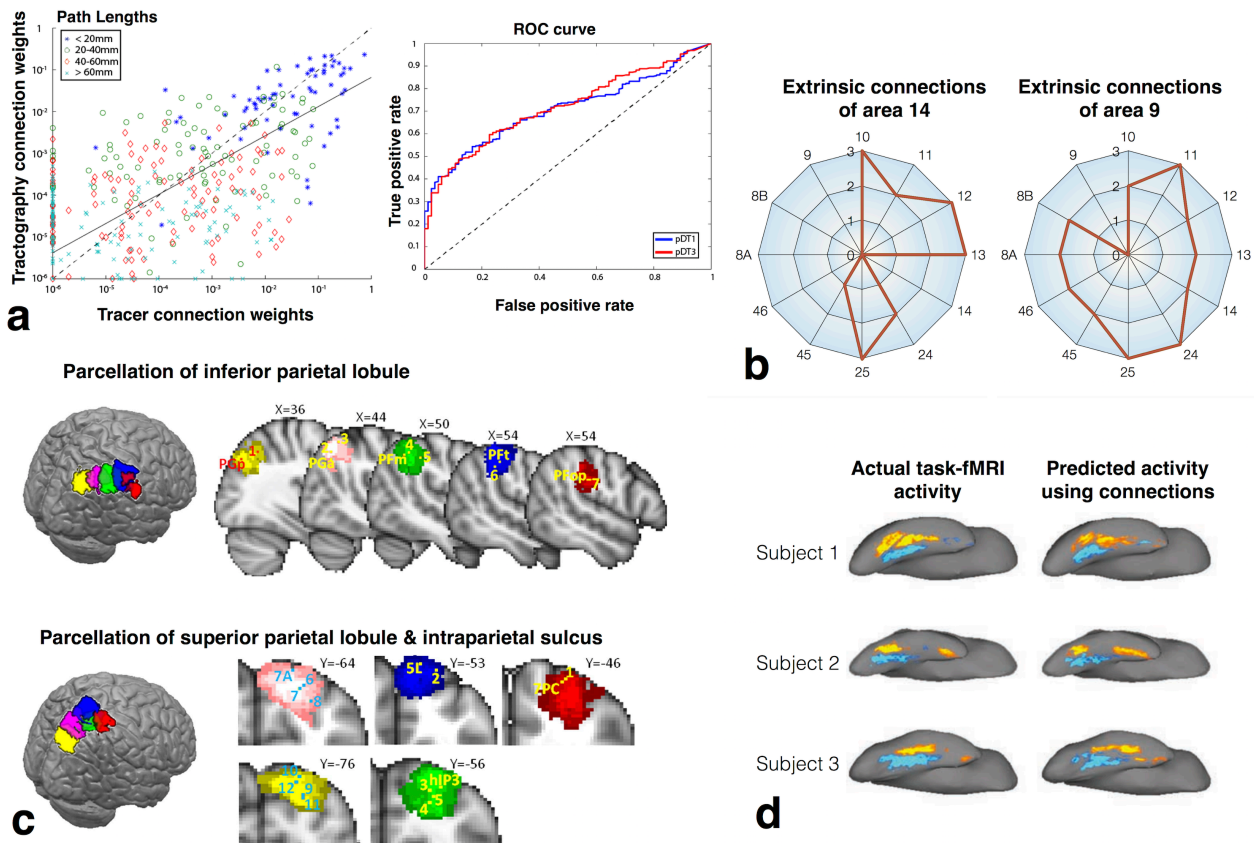
Figure 5. a) Correlation between connection weights inferred from tracers and tractography in the macaque connectome (correlation coefficient r~0.55) [23]. Shorter connections contribute to the correlation more than the longer. Receiver operating characteristic (ROC) curves for two alternative tractography algorithms, as benchmarked against a ground truth derived from tracers. An area under the curve of ~0.72 suggests that tractography does better than chance, but it is far from perfect. b) Connectivity fingerprints of two functionally distinct prefrontal areas, as measured using tracers in the macaque brain and presented in [4]. The radial distance represents connection strength (weak=1, medium/ambiguous strength=2, strong=3). c) Two parcellations of the parietal cortex based on the "connectivity fingerprints" methodology, as estimated by in-vivo tractography in humans [44]. For each case, sagittal (or coronal) views of the parcels are shown superimposed with the centre of gravity of cytoarchitectonic regions and center of mass of fMRI activations in various relevant tasks. The functional relevance of these parcels is demonstrated by the marked overlap. d) Predicting activity in the face area of the fusiform gyrus with a model that uses only the pattern of extrinsic connections of the fusiform gyrus to the rest of the brain [5]. The actual activity measured using task fMRI is also shown for comparison. Notice how individual variability in activation during task is predicted by the respective individual variability in the connections. All panels are reproduced with permission.
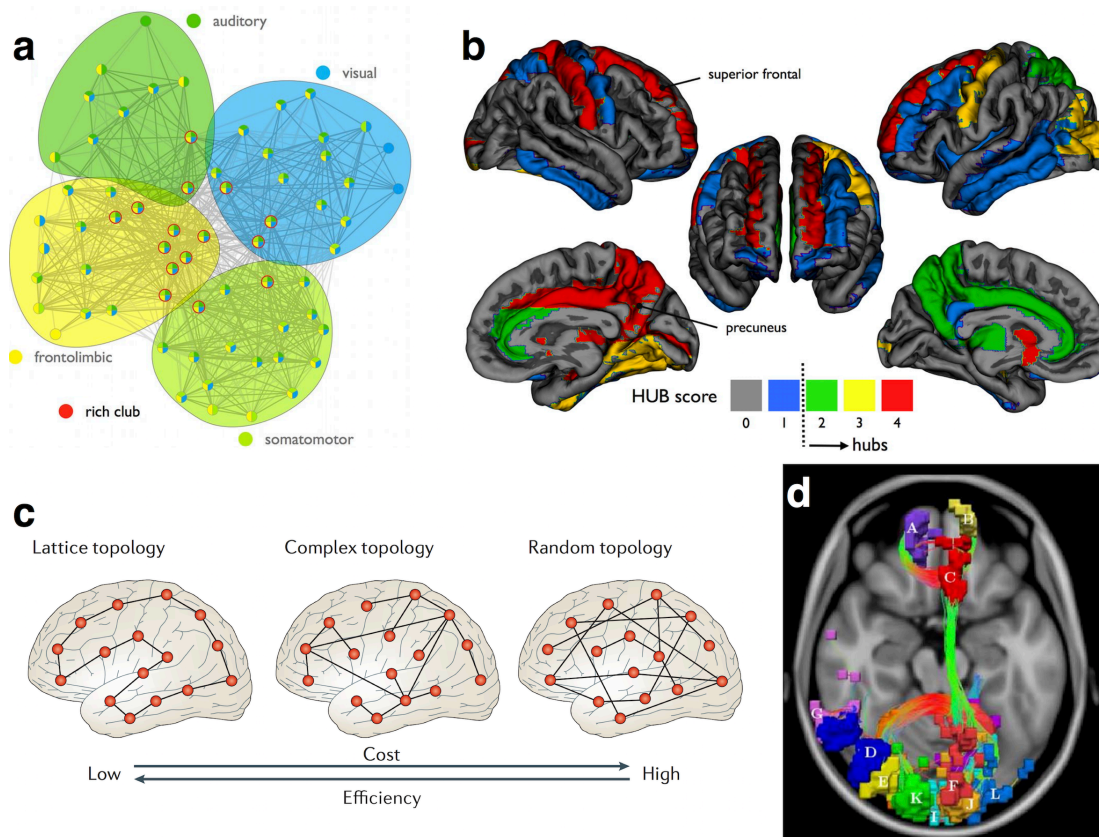
Figure 6. Characteristic network properties of brain graphs. a) Brain graphs are modular networks. In this example, each of the four modules is encapsulated by a distinctly coloured bubble and comprises a densely interconnected set of cortical regions that perform a specialized function. The four modules are interconnected by a network of hub nodes (outlined in red) that form a rich club. Cortical regions in distinct modules most often communicate via routes traversing the rich club. The modules shown have been delineated in the cat connectome reconstructed with tract tracing. b) Hub nodes of the human connectome. Hub scores represent consistency across measures of node degree and centrality. Hub nodes are convergence and divergence points of neural information. c) Network economy refers to the trade-off between network cost and network efficiency. Brains graphs are complex networks that attain a trade-off between the low cost of lattice networks and the high efficiency of random networks. The addition of a small number of long-distance connections to a lattice network results in a small increase in network cost, but a substantial reduction in the average number of connections that need to be traversed to establish a route between pairs of nodes. d) Network of disrupted connections comprising significantly fewer streamlines in patients with schizophrenia compared to healthy individuals. Each of the coloured regions represents a node. Streamlines are only shown for disrupted connections. The cingulum bundle, genu and splenium of the corpus callosum can be seen to be disrupted. Panel (a) reproduced from [251], (b) from [128], (c) from [228] and (d) from [219] with permission.

References

1.   Neubert, F.X., R.B. Mars, E.R. Buch, E. Olivier, and M.F. Rushworth. Cortical and subcortical interactions during action reprogramming and their related white matter pathways. *Proc Natl Acad Sci U S A*, 107(30): 13240-5, 2010.
2.   Dubois, J., G. Dehaene-Lambertz, S. Kulikova, C. Poupon, P.S. Huppi, and L. Hertz-Pannier. The early development of brain white matter: a review of imaging studies in fetuses, newborns and infants. *Neuroscience*, 276: 48-71, 2014.
3.   Scholz, J., M.C. Klein, T.E. Behrens, and H. Johansen-Berg. Training induces changes in white-matter architecture. *Nat Neurosci*, 12(11): 1370-1, 2009.
4.   Passingham, R.E., K.E. Stephan, and R. Kotter. The anatomical basis of functional localization in the cortex. *Nat Rev Neurosci*, 3(8): 606-16, 2002.
5.   Saygin, Z.M., D.E. Osher, K. Koldewyn, G. Reynolds, J.D. Gabrieli, and R.R. Saxe. Anatomical connectivity patterns predict face selectivity in the fusiform gyrus. *Nat Neurosci*, 15(2): 321-7, 2012.
6.   Behrens, T.E. and O. Sporns. Human connectomics. *Curr Opin Neurobiol*, 22(1): 144-53, 2012.
7.   Sporns, O., G. Tononi, and R. Kotter. The human connectome: A structural description of the human brain. *PLoS Comput Biol*, 1(4): e42, 2005.
8.   Hagmann, P., L. Cammoun, X. Gigandet, R. Meuli, C.J. Honey, V.J. Wedeen, and O. Sporns. Mapping the structural core of human cerebral cortex. *PLoS Biol*, 6(7): e159, 2008.
9.   Passingham, R.E. What we can and cannot tell about the wiring of the human brain. *Neuroimage*, 80: 14-7, 2013.
10.   Griffa, A., P.S. Baumann, J.P. Thiran, and P. Hagmann. Structural connectomics in brain diseases. *Neuroimage*, 80: 515-26, 2013.
11.   Axer, H. Invasive Methods for Tracing White Matter Architecture, in *Diffusion MRI: Theory, Methods and Applications*, D.K. Jones, Editor Oxford University Press, 31-42, 2011.
12.   Lichtman, J.W., J. Livet, and J.R. Sanes. A technicolour approach to the connectome. *Nat Rev Neurosci*, 9(6): 417-22, 2008.
13.   Mahou, P., M. Zimmerley, K. Loulier, K.S. Matho, G. Labroille, X. Morin, W. Supatto, J. Livet, D. Debarre, and E. Beaurepaire. Multicolor two-photon tissue imaging by wavelength mixing. *Nat Methods*, 9(8): 815-8, 2012.
14.   Denk, W. and H. Horstmann. Serial block-face scanning electron microscopy to reconstruct three-dimensional tissue nanostructure. *PLoS Biol*, 2(11): e329, 2004.
15.   Economo, M.N., N.G. Clack, L.D. Lavis, C.R. Gerfen, K. Svoboda, E.W. Myers, and J. Chandrashekar. A platform for brain-wide imaging and reconstruction of individual neurons. *Elife*, 5: e10566, 2016.
16.   White, J.G., E. Southgate, J.N. Thomson, and S. Brenner. The structure of the nervous system of the nematode Caenorhabditis elegans. *Philos Trans R Soc Lond B Biol Sci*, 314(1165): 1-340, 1986.
17.   Jbabdi, S., S.N. Sotiropoulos, S.N. Haber, D.C. Van Essen, and T.E. Behrens. Measuring macroscopic brain connections in vivo. *Nat Neurosci*, 18(11): 1546-55, 2015.

18.   Felleman, D.J. and D.C. Van Essen. Distributed hierarchical processing in the primate cerebral cortex. *Cereb Cortex*, 1(1): 1-47, 1991.

19.   Markov, N.T., M.M. Ercsey-Ravasz, A.R. Ribeiro Gomes, C. Lamy, L. Magrou, J. Vezoli, P. Misery, A. Falchier, R. Quilodran, M.A. Gariel, J. Sallet, R. Gamanut, C. Huissoud, S. Clavagnier, P. Giroud, D. Sappey-Marinier, P. Barone, C. Dehay, Z. Toroczkai, K. Knoblauch, D.C. Van Essen, and H. Kennedy. A weighted and directed interareal connectivity matrix for macaque cerebral cortex. *Cereb Cortex*, 24(1): 17-36, 2014.

20.   Oh, S.W., J.A. Harris, L. Ng, B. Winslow, N. Cain, S. Mihalas, Q. Wang, C. Lau, L. Kuan, A.M. Henry, M.T. Mortrud, B. Ouellette, T.N. Nguyen, S.A. Sorensen, C.R. Slaughterbeck, W. Wakeman, Y. Li, D. Feng, A. Ho, E. Nicholas, K.E. Hirokawa, P. Bohn, K.M. Joines, H. Peng, M.J. Hawrylycz, J.W. Phillips, J.G. Hohmann, P. Wohnoutka, C.R. Gerfen, C. Koch, A. Bernard, C. Dang, A.R. Jones, and H. Zeng. A mesoscale connectome of the mouse brain. *Nature*, 508(7495): 207-14, 2014.

21.   Stephan, K.E. The history of CoCoMac. *Neuroimage*, 80: 46-52, 2013.

22.   Scannell, J.W., C. Blakemore, and M.P. Young. Analysis of connectivity in the cat cerebral cortex. *J Neurosci*, 15(2): 1463-83, 1995.

23.   Donahue, C.J., S.N. Sotiropoulos, S. Jbabdi, M. Hernandez-Fernandez, T.E. Behrens, T.B. Dyrby, T. Coalson, D. Kennedy, K. Knoblauch, D.C. Van Essen, and M.F. Glasser. Using Diffusion Tractography to Predict Cortical Connection Strength and Distance: A Quantitative Comparison with Tracers in the Monkey. *J Neurosci*, 36(25): 6758-6770, 2016.

24.   Catani, M., R.J. Howard, S. Pajevic, and D.K. Jones. Virtual in vivo interactive dissection of white matter fasciculi in the human brain. *Neuroimage*, 17(1): 77-94, 2002.

25.   Jones, D.K., T.R. Knosche, and R. Turner. White matter integrity, fiber count, and other fallacies: the do's and don'ts of diffusion MRI. *Neuroimage*, 73: 239-54, 2013.

26.   Schuz, A.B.V. The human cortical white matter: quantitative aspects of cortico-cortical long-range connectivity, in *Cortical Areas: Unity and Diversity*, A. Shuez and R. Miller, Editors, Taylor & Francis: London, 377-384, 2002.

27.   Van Essen, D.C., S. Jbabdi, S.N. Sotiropoulos, C. Chen, K. Dikranian, T. Coalson, J. Harwell, T.E.J. Behrens, and M.F. Glasser. Mapping connections in humans and nonhuman primates: Aspirations and challenges for diffusion imaging, in *Diffusion MRI: From quantitative measurement to in-vivo neuroanatomy (2nd edition)*, H. Johansen-Berg and T.E. Behrens, Editors, Elsevier, 337-358, 2013.

28.   Craddock, R.C., S. Jbabdi, C.G. Yan, J.T. Vogelstein, F.X. Castellanos, A. Di Martino, C. Kelly, K. Heberlein, S. Colcombe, and M.P. Milham. Imaging human connectomes at the macroscale. *Nat Methods*, 10(6): 524-39, 2013.

29.   Caspers, S., S.B. Eickhoff, K. Zilles, and K. Amunts. Microstructural grey matter parcellation and its relevance for connectome analyses. *Neuroimage*, 80: 18-26, 2013.

30.   Tzourio-Mazoyer, N., B. Landeau, D. Papathanassiou, F. Crivello, O. Etard, N. Delcroix, B. Mazoyer, and M. Joliot. Automated anatomical labeling of activations in SPM using a macroscopic anatomical parcellation of the MNI MRI single-subject brain. *Neuroimage*, 15(1): 273-89, 2002.

31.   Desikan, R.S., F. Segonne, B. Fischl, B.T. Quinn, B.C. Dickerson, D. Blacker, R.L. Buckner, A.M. Dale, R.P. Maguire, B.T. Hyman, M.S. Albert, and R.J. Killiany. An automated labeling system for subdividing the human cerebral cortex on MRI scans into gyral based regions of interest. *Neuroimage*, 31(3): 968-80, 2006.

32.   Lancaster, J.L., M.G. Woldorff, L.M. Parsons, M. Liotti, C.S. Freitas, L. Rainey, P.V. Kochunov, D. Nickerson, S.A. Mikiten, and P.T. Fox. Automated Talairach atlas labels for functional brain mapping. *Hum Brain Mapp*, 10(3): 120-31, 2000.

33.   Eickhoff, S.B., K.E. Stephan, H. Mohlberg, C. Grefkes, G.R. Fink, K. Amunts, and K. Zilles. A new SPM toolbox for combining probabilistic cytoarchitectonic maps and functional imaging data. *Neuroimage*, 25(4): 1325-35, 2005.

34.   Yeo, B.T., F.M. Krienen, J. Sepulcre, M.R. Sabuncu, D. Lashkari, M. Hollinshead, J.L. Roffman, J.W. Smoller, L. Zollei, J.R. Polimeni, B. Fischl, H. Liu, and R.L. Buckner. The organization of the human cerebral cortex estimated by intrinsic functional connectivity. *J Neurophysiol*, 106(3): 1125-65, 2011.

35.   Smith, S.M., P.T. Fox, K.L. Miller, D.C. Glahn, P.M. Fox, C.E. Mackay, N. Filippini, K.E. Watkins, R. Toro, A.R. Laird, and C.F. Beckmann. Correspondence of the brain's functional architecture during activation and rest. *Proc Natl Acad Sci U S A*, 106(31): 13040-5, 2009.

36.   Craddock, R.C., G.A. James, P.E. Holtzheimer, 3rd, X.P. Hu, and H.S. Mayberg. A whole brain fMRI atlas generated via spatially constrained spectral clustering. *Hum Brain Mapp*, 33(8): 1914-28, 2012.

37.   Thirion, B., G. Varoquaux, E. Dohmatob, and J.B. Poline. Which fMRI clustering gives good brain parcellations? *Front Neurosci*, 8: 167, 2014.

38.   Cohen, A.L., D.A. Fair, N.U. Dosenbach, F.M. Miezin, D. Dierker, D.C. Van Essen, B.L. Schlaggar, and S.E. Petersen. Defining functional areas in individual human brains using resting functional connectivity MRI. *Neuroimage*, 41(1): 45-57, 2008.

39.   Glasser, M.F., T. Coalson, E.C. Robinson, C.D. Hacker, J. Harwell, E. Yacoub, K. Ugurbil, J. Andersson, C.F. Beckmann, M. Jenkinson, S. Smith, and D.C. Van Essen. A multi-modal parcellation of human cerebral cortex. *Nature*, In press, 2016.

40.   Fan, L., H. Li, J. Zhuo, Y. Zhang, J. Wang, L. Chen, Z. Yang, C. Chu, S. Xie, A.R. Laird, P.T. Fox, S.B. Eickhoff, C. Yu, and T. Jiang. The Human Brainnetome Atlas: A New Brain Atlas Based on Connectional Architecture. *Cereb Cortex*, 2016.

41.   Beckmann, M., H. Johansen-Berg, and M.F. Rushworth. Connectivity-based parcellation of human cingulate cortex and its relation to functional specialization. *J Neurosci*, 29(4): 1175-90, 2009.

42.   Behrens, T.E., H. Johansen-Berg, M.W. Woolrich, S.M. Smith, C.A. Wheeler-Kingshott, P.A. Boulby, G.J. Barker, E.L. Sillery, K. Sheehan, O. Ciccarelli, A.J. Thompson, J.M. Brady, and P.M. Matthews. Non-invasive mapping of connections between human thalamus and cortex using diffusion imaging. *Nat Neurosci*, 6(7): 750-7, 2003.

43.   Johansen-Berg, H., T.E. Behrens, M.D. Robson, I. Drobnjak, M.F. Rushworth, J.M. Brady, S.M. Smith, D.J. Higham, and P.M. Matthews.

Changes in connectivity profiles define functionally distinct regions in human medial frontal cortex. *Proc Natl Acad Sci U S A*, 101(36): 13335-40, 2004.

44. Mars, R.B., S. Jbabdi, J. Sallet, J.X. O'Reilly, P.L. Croxson, E. Olivier, M.P. Noonan, C. Bergmann, A.S. Mitchell, M.G. Baxter, T.E. Behrens, H. Johansen-Berg, V. Tomassini, K.L. Miller, and M.F. Rushworth. Diffusion-weighted imaging tractography-based parcellation of the human parietal cortex and comparison with human and macaque resting-state functional connectivity. *J Neurosci*, 31(11): 4087-100, 2011.

45. Eickhoff, S.B., B. Thirion, G. Varoquaux, and D. Bzdok. Connectivity-based parcellation: Critique and implications. *Hum Brain Mapp*, 36(12): 4771-92, 2015.

46. Van Essen, D.C. Cartography and connectomes. *Neuron*, 80(3): 775-90, 2013.

47. Amunts, K., A. Malikovic, H. Mohlberg, T. Schormann, and K. Zilles. Brodmann's areas 17 and 18 brought into stereotaxic space-where and how variable? *Neuroimage*, 11(1): 66-84, 2000.

48. Fischl, B., N. Rajendran, E. Busa, J. Augustinack, O. Hinds, B.T. Yeo, H. Mohlberg, K. Amunts, and K. Zilles. Cortical folding patterns and predicting cytoarchitecture. *Cereb Cortex*, 18(8): 1973-80, 2008.

49. Robinson, E.C., S. Jbabdi, M.F. Glasser, J. Andersson, G.C. Burgess, M.P. Harms, S.M. Smith, D.C. Van Essen, and M. Jenkinson. MSM: a new flexible framework for Multimodal Surface Matching. *Neuroimage*, 100: 414-26, 2014.

50. Jbabdi, S., S.N. Sotiropoulos, and T.E. Behrens. The topographic connectome. *Curr Opin Neurobiol*, 23(2): 207-15, 2013.

51. Bassett, D.S., J.A. Brown, V. Deshpande, J.M. Carlson, and S.T. Grafton. Conserved and variable architecture of human white matter connectivity. *Neuroimage*, 54(2): 1262-79, 2011.

52. Da Mota, B., V. Fritsch, G. Varoquaux, T. Banaschewski, G.J. Barker, A.L. Bokde, U. Bromberg, P. Conrod, J. Gallinat, H. Garavan, J.L. Martinot, F. Nees, T. Paus, Z. Pausova, M. Rietschel, M.N. Smolka, A. Strohle, V. Frouin, J.B. Poline, B. Thirion, and I. consortium. Randomized parcellation based inference. *Neuroimage*, 89: 203-15, 2014.

53. Zalesky, A., A. Fornito, I.H. Harding, L. Cocchi, M. Yucel, C. Pantelis, and E.T. Bullmore. Whole-brain anatomical networks: does the choice of nodes matter? *Neuroimage*, 50(3): 970-83, 2010.

54. Cammoun, L., X. Gigandet, D. Meskaldji, J.P. Thiran, O. Sporns, K.Q. Do, P. Maeder, R. Meuli, and P. Hagmann. Mapping the human connectome at multiple scales with diffusion spectrum MRI. *J Neurosci Methods*, 203(2): 386-97, 2012.

55. Chen, H., T. Liu, Y. Zhao, T. Zhang, Y. Li, M. Li, H. Zhang, H. Kuang, L. Guo, J.Z. Tsien, and T. Liu. Optimization of large-scale mouse brain connectome via joint evaluation of DTI and neuron tracing data. *Neuroimage*, 115: 202-13, 2015.

56. Calabrese, E., A. Badea, G. Cofer, Y. Qi, and G.A. Johnson. A Diffusion MRI Tractography Connectome of the Mouse Brain and Comparison with Neuronal Tracer Data. *Cereb Cortex*, 25(11): 4628-37, 2015.

57. Gao, Y., A.S. Choe, I. Stepniewska, X. Li, M.J. Avison, and A.W. Anderson. Validation of DTI tractography-based measures of primary motor area connectivity in the squirrel monkey brain. *PLoS One*, 8(10): e75065, 2013.

58.   Alexander-Bloch, A., J.N. Giedd, and E. Bullmore. Imaging structural co-variance between human brain regions. *Nat Rev Neurosci*, 14(5): 322-36, 2013.

59.   Behrens, T.E. and S. Jbabdi. MR Diffusion Tractography, in *Diffusion MRI: From quantitative measurement to in-vivo neuroanatomy*, H. Johansen-Berg and T.E. Behrens, Editors, Elsevier, 333-351, 2009.

60.   Jbabdi, S. and H. Johansen-Berg. Tractography: where do we go from here? *Brain Connect*, 1(3): 169-83, 2011.

61.   Tournier, J.D., S. Mori, and A. Leemans. Diffusion tensor imaging and beyond. *Magn Reson Med*, 65(6): 1532-56, 2011.

62.   Seunarine, K.K. and D.C. Alexander. Multiple fibers: Beyond the diffusion tensor, in *Diffusion MRI: From quantitative measurement to in-vivo neuroanatomy*, H. Johansen-Berg and T.E. Behrens, Editors, Elsevier, 55-72, 2009.

63.   Basser, P.J., S. Pajevic, C. Pierpaoli, J. Duda, and A. Aldroubi. In vivo fiber tractography using DT-MRI data. *Magn Reson Med*, 44(4): 625-32, 2000.

64.   Catani, M. and M. Thiebaut de Schotten. A diffusion tensor imaging tractography atlas for virtual in vivo dissections. *Cortex*, 44(8): 1105-32, 2008.

65.   Basser, P.J., J. Mattiello, and D. LeBihan. Estimation of the effective self-diffusion tensor from the NMR spin echo. *J Magn Reson B*, 103(3): 247-54, 1994.

66.   Kaden, E., T.R. Knosche, and A. Anwander. Parametric spherical deconvolution: inferring anatomical connectivity using diffusion MR imaging. *Neuroimage*, 37(2): 474-88, 2007.

67.   Anderson, A.W. Measurement of fiber orientation distributions using high angular resolution diffusion imaging. *Magn Reson Med*, 54(5): 1194-206, 2005.

68.   Dell'Acqua, F., G. Rizzo, P. Scifo, R.A. Clarke, G. Scotti, and F. Fazio. A model-based deconvolution approach to solve fiber crossing in diffusion-weighted MR imaging. *IEEE Trans Biomed Eng*, 54(3): 462-72, 2007.

69.   Tournier, J.D., F. Calamante, D.G. Gadian, and A. Connelly. Direct estimation of the fiber orientation density function from diffusion-weighted MRI data using spherical deconvolution. *Neuroimage*, 23(3): 1176-85, 2004.

70.   Descoteaux, M., R. Deriche, T.R. Knosche, and A. Anwander. Deterministic and probabilistic tractography based on complex fibre orientation distributions. *IEEE Trans Med Imaging*, 28(2): 269-86, 2009.

71.   Alexander, D.C. Maximum entropy spherical deconvolution for diffusion MRI. *Inf Process Med Imaging*, 19: 76-87, 2005.

72.   Tuch, D.S. Q-ball imaging. *Magn Reson Med*, 52(6): 1358-72, 2004.

73.   Wedeen, V.J., P. Hagmann, W.Y. Tseng, T.G. Reese, and R.M. Weisskoff. Mapping complex tissue architecture with diffusion spectrum magnetic resonance imaging. *Magn Reson Med*, 54(6): 1377-86, 2005.

74.   Behrens, T.E., H.J. Berg, S. Jbabdi, M.F. Rushworth, and M.W. Woolrich. Probabilistic diffusion tractography with multiple fibre orientations: What can we gain? *Neuroimage*, 34(1): 144-55, 2007.

75.   Tournier, J.D., F. Calamante, and A. Connelly. Robust determination of the fibre orientation distribution in diffusion MRI: non-negativity constrained super-resolved spherical deconvolution. *Neuroimage*, 35(4): 1459-72, 2007.

76.	Tuch, D.S., T.G. Reese, M.R. Wiegell, and V.J. Wedeen. Diffusion MRI of complex neural architecture. *Neuron*, 40(5): 885-95, 2003.

77.	Bastiani, M., N.J. Shah, R. Goebel, and A. Roebroeck. Human cortical connectome reconstruction from diffusion weighted MRI: the effect of tractography algorithm. *Neuroimage*, 62(3): 1732-49, 2012.

78.	Fillard, P., M. Descoteaux, A. Goh, S. Gouttard, B. Jeurissen, J. Malcolm, A. Ramirez-Manzanares, M. Reisert, K. Sakaie, F. Tensaouti, T. Yo, J.F. Mangin, and C. Poupon. Quantitative evaluation of 10 tractography algorithms on a realistic diffusion MR phantom. *Neuroimage*, 56(1): 220-34, 2011.

79.	Schilling, K., V. Janve, Y. Gao, I. Stepniewska, B. Landman, and A. Anderson. Comparing Diffusion MRI with the Fiber Architecture and Tract Density of Gyral Blades. in *ISMRM Proceesings*, Signapore: 924, 2016.

80.	Behrens, T.E., M.W. Woolrich, M. Jenkinson, H. Johansen-Berg, R.G. Nunes, S. Clare, P.M. Matthews, J.M. Brady, and S.M. Smith. Characterization and propagation of uncertainty in diffusion-weighted MR imaging. *Magn Reson Med*, 50(5): 1077-88, 2003.

81.	Mori, S., B.J. Crain, V.P. Chacko, and P.C. van Zijl. Three-dimensional tracking of axonal projections in the brain by magnetic resonance imaging. *Ann Neurol*, 45(2): 265-9, 1999.

82.	Parker, G.J., H.A. Haroon, and C.A. Wheeler-Kingshott. A framework for a streamline-based probabilistic index of connectivity (PICo) using a structural interpretation of MRI diffusion measurements. *J Magn Reson Imaging*, 18(2): 242-54, 2003.

83.	Campbell, J.S., K. Siddiqi, V.V. Rymar, A.F. Sadikot, and G.B. Pike. Flow-based fiber tracking with diffusion tensor and q-ball data: validation and comparison to principal diffusion direction techniques. *Neuroimage*, 27(4): 725-36, 2005.

84.	Fillard, P., C. Poupon, and J.F. Mangin. A novel global tractography algorithm based on an adaptive spin glass model. *Med Image Comput Comput Assist Interv*, 12(Pt 1): 927-34, 2009.

85.	Iturria-Medina, Y., E.J. Canales-Rodriguez, L. Melie-Garcia, P.A. Valdes-Hernandez, E. Martinez-Montes, Y. Aleman-Gomez, and J.M. Sanchez-Bornot. Characterizing brain anatomical connections using diffusion weighted MRI and graph theory. *Neuroimage*, 36(3): 645-60, 2007.

86.	Jbabdi, S., M.W. Woolrich, J.L. Andersson, and T.E. Behrens. A Bayesian framework for global tractography. *Neuroimage*, 37(1): 116-29, 2007.

87.	Kreher, B.W., I. Mader, and V.G. Kiselev. Gibbs tracking: a novel approach for the reconstruction of neuronal pathways. *Magn Reson Med*, 60(4): 953-63, 2008.

88.	Reisert, M., I. Mader, C. Anastasopoulos, M. Weigel, S. Schnell, and V. Kiselev. Global fiber reconstruction becomes practical. *Neuroimage*, 54(2): 955-62, 2011.

89.	Sotiropoulos, S.N., L. Bai, P.S. Morgan, C.S. Constantinescu, and C.R. Tench. Brain tractography using Q-ball imaging and graph theory: Improved connectivities through fibre crossings via a model-based approach. *Neuroimage*, 49(3): 2444-56, 2010.

90.	Iturria-Medina, Y., A. Perez Fernandez, D.M. Morris, E.J. Canales-Rodriguez, H.A. Haroon, L. Garcia Penton, M. Augath, L. Galan Garcia, N. Logothetis,

G.J. Parker, and L. Melie-Garcia. Brain hemispheric structural efficiency and interconnectivity rightward asymmetry in human and nonhuman primates. *Cereb Cortex*, 21(1): 56-67, 2011.

91. Jones, D.K. Tractography gone wild: probabilistic fibre tracking using the wild bootstrap with diffusion tensor MRI. *IEEE Trans Med Imaging*, 27(9): 1268-74, 2008.

92. Jeurissen, B., A. Leemans, D.K. Jones, J.D. Tournier, and J. Sijbers. Probabilistic fiber tracking using the residual bootstrap with constrained spherical deconvolution. *Hum Brain Mapp*, 32(3): 461-79, 2011.

93. Bonilha, L., E. Gleichgerrcht, J. Fridriksson, C. Rorden, J.L. Breedlove, T. Nesland, W. Paulus, G. Helms, and N.K. Focke. Reproducibility of the Structural Brain Connectome Derived from Diffusion Tensor Imaging. *PLoS One*, 10(8): e0135247, 2015.

94. Buchanan, C.R., C.R. Pernet, K.J. Gorgolewski, A.J. Storkey, and M.E. Bastin. Test-retest reliability of structural brain networks from diffusion MRI. *Neuroimage*, 86: 231-43, 2014.

95. Prckovska, V., P. Rodrigues, A. Puigdellivol Sanchez, M. Ramos, M. Andorra, E. Martinez-Heras, C. Falcon, A. Prats-Galino, and P. Villoslada. Reproducibility of the Structural Connectome Reconstruction across Diffusion Methods. *J Neuroimaging*, 26(1): 46-57, 2016.

96. Zalesky, A., A. Fornito, L. Cocchi, L.L. Gollo, M.P. van den Heuvel, and M. Breakspear. Connectome sensitivity or specificity: which is more important? *Neuroimage*, 142: 407-420, 2016.

97. Cote, M.A., G. Girard, A. Bore, E. Garyfallidis, J.C. Houde, and M. Descoteaux. Tractometer: towards validation of tractography pipelines. *Med Image Anal*, 17(7): 844-57, 2013.

98. Li, L., J.K. Rilling, T.M. Preuss, M.F. Glasser, and X. Hu. The effects of connection reconstruction method on the interregional connectivity of brain networks via diffusion tractography. *Hum Brain Mapp*, 33(8): 1894-913, 2012.

99. Wakana, S., H. Jiang, L.M. Nagae-Poetscher, P.C. van Zijl, and S. Mori. Fiber tract-based atlas of human white matter anatomy. *Radiology*, 230(1): 77-87, 2004.

100. Girard, G., K. Whittingstall, R. Deriche, and M. Descoteaux. Towards quantitative connectivity analysis: reducing tractography biases. *Neuroimage*, 98: 266-78, 2014.

101. Smith, R.E., J.D. Tournier, F. Calamante, and A. Connelly. Anatomically-constrained tractography: improved diffusion MRI streamlines tractography through effective use of anatomical information. *Neuroimage*, 62(3): 1924-38, 2012.

102. Smith, R.E., J.D. Tournier, F. Calamante, and A. Connelly. The effects of SIFT on the reproducibility and biological accuracy of the structural connectome. *Neuroimage*, 104: 253-65, 2015.

103. Sotiropoulos, S.N., T.E. Behrens, and S. Jbabdi. Ball and rackets: Inferring fiber fanning from diffusion-weighted MRI. *Neuroimage*, 60(2): 1412-25, 2012.

104. Seunarine, K.K., P.A. Cook, M.G. Hall, K.V. Embleton, G.J.M. Parker, and D.C. Alexander. Exploiting peak anisotropy for tracking through complex structures. in *ICCV Proceedings*, Rio de Janeiro, Brazil, 2007.

105. Savadjiev, P., J.S. Campbell, G.B. Pike, and K. Siddiqi. 3D curve inference for diffusion MRI regularization and fibre tractography. *Med Image Anal*, 10(5): 799-813, 2006.
106. Barmpoutis, A., B.C. Vemuri, D. Howland, and J.R. Forder. Extracting tractosemas from a displacement probability field for tractography in DW-MRI. *Med Image Comput Comput Assist Interv*, 11(Pt 1): 9-16, 2008.
107. Pestilli, F., J.D. Yeatman, A. Rokem, K.N. Kay, and B.A. Wandell. Evaluation and statistical inference for human connectomes. *Nat Methods*, 11(10): 1058-63, 2014.
108. Smith, R.E., J.D. Tournier, F. Calamante, and A. Connelly. SIFT: Spherical-deconvolution informed filtering of tractograms. *Neuroimage*, 67: 298-312, 2013.
109. Reisert, M., E. Kellner, and V.G. Kiselev. About the geometry of asymmetric fiber orientation distributions. *IEEE Trans Med Imaging*, 31(6): 1240-9, 2012.
110. Rowe, M., H. Zhang, and D.C. Alexander. Beyond Crossing Fibers: Tractography Exploiting Sub-voxel Fibre Dispersion and Neighbourhood Structure. in *IPMI*, Asilomar, CA: 402-413, 2013.
111. Savadjiev, P., J.S. Campbell, M. Descoteaux, R. Deriche, G.B. Pike, and K. Siddiqi. Labeling of ambiguous subvoxel fibre bundle configurations in high angular resolution diffusion MRI. *Neuroimage*, 41(1): 58-68, 2008.
112. Bastiani, M., M. Cottaar, K. Dikranian, A. Ghosh, H. Zhang, D.C. Alexander, T. Behrens, S. Jbabdi, and S.N. Sotiropoulos. Improved tractography using asymmetric fibre orientation distributions. *NeuroImage*, 2017.
113. Reisert, M., V.G. Kiselev, B. Dihtal, E. Kellner, and D.S. Novikov. MesoFT: unifying diffusion modelling and fiber tracking. *Med Image Comput Comput Assist Interv*, 17(Pt 3): 201-8, 2014.
114. Sherbondy, A.J., M.C. Rowe, and D.C. Alexander. MicroTrack: an algorithm for concurrent projectome and microstructure estimation. *Med Image Comput Comput Assist Interv*, 13(Pt 1): 183-90, 2010.
115. Daducci, A., A. Dal Palu, M. Descoteaux, and J.P. Thiran. Microstructure Informed Tractography: Pitfalls and Open Challenges. *Front Neurosci*, 10: 247, 2016.
116. Girard, G., F. Rutger, M. Descoteaux, R. Deriche, and D. Wassermann. AxTract: Microstructure-Driven Tractography Based on the Ensemble Average Propagator. *Inf Process Med Imaging*, 24: 675-86, 2015.
117. Markov, N.T., J. Vezoli, P. Chameau, A. Falchier, R. Quilodran, C. Huissoud, C. Lamy, P. Misery, P. Giroud, S. Ullman, P. Barone, C. Dehay, K. Knoblauch, and H. Kennedy. Anatomy of hierarchy: feedforward and feedback pathways in macaque visual cortex. *J Comp Neurol*, 522(1): 225-59, 2014.
118. Leuze, C.W., A. Anwander, P.L. Bazin, B. Dhital, C. Stuber, K. Reimann, S. Geyer, and R. Turner. Layer-specific intracortical connectivity revealed with diffusion MRI. *Cereb Cortex*, 24(2): 328-39, 2014.
119. Barazany, D. and Y. Assaf. Visualization of cortical lamination patterns with magnetic resonance imaging. *Cereb Cortex*, 22(9): 2016-23, 2012.
120. Tziortzi, A.C., S.N. Haber, G.E. Searle, C. Tsoumpas, C.J. Long, P. Shotbolt, G. Douaud, S. Jbabdi, T.E. Behrens, E.A. Rabiner, M. Jenkinson, and R.N. Gunn. Connectivity-based functional analysis of dopamine release in the

striatum using diffusion-weighted MRI and positron emission tomography. *Cereb Cortex*, 24(5): 1165-77, 2014.

121. Glasser, M.F., S.M. Smith, D.S. Marcus, J. Andersson, E.J. Auerbach, T.E. Behrens, T.S. Coalson, M.P. Harms, M. Jenkinson, S. Moeller, E.C. Robinson, S.N. Sotiropoulos, J. Xu, E. Yacoub, K. Ugurbil, and D.C. Van Essen. The Human Connectome Project's neuroimaging approach. *Nature Neuroscience* 19(9): 1175-1187, 2016.

122. Reveley, C., A.K. Seth, C. Pierpaoli, A.C. Silva, D. Yu, R.C. Saunders, D.A. Leopold, and F.Q. Ye. Superficial white matter fiber systems impede detection of long-range cortical connections in diffusion MR tractography. *Proc Natl Acad Sci U S A*, 112(21): E2820-8, 2015.

123. Yo, T.S., A. Anwander, M. Descoteaux, P. Fillard, C. Poupon, and T.R. Knosche. Quantifying brain connectivity: a comparative tractography study. *Med Image Comput Comput Assist Interv*, 12(Pt 1): 886-93, 2009.

124. Van den Heuvel, M.P., M.A. de Reus, L. Feldman Barrett, L.H. Scholtens, F.M. Coopmans, R. Schmidt, T.M. Preuss, J.K. Rilling, and L. Li. Comparison of diffusion tractography and tract-tracing measures of connectivity strength in rhesus macaque connectome. *Hum Brain Mapp*, 36(8): 3064-75, 2015.

125. Lemkaddem, A., A. Daducci, N. Kunz, F. Lazeyras, M. Seeck, J.P. Thiran, and S. Vulliemoz. Connectivity and tissue microstructural alterations in right and left temporal lobe epilepsy revealed by diffusion spectrum imaging. *Neuroimage Clin*, 5: 349-58, 2014.

126. Hagmann, P., O. Sporns, N. Madan, L. Cammoun, R. Pienaar, V.J. Wedeen, R. Meuli, J.P. Thiran, and P.E. Grant. White matter maturation reshapes structural connectivity in the late developing human brain. *Proc Natl Acad Sci U S A*, 107(44): 19067-72, 2010.

127. Mandl, R.C., H.G. Schnack, J. Luigjes, M.P. van den Heuvel, W. Cahn, R.S. Kahn, and H.E. Hulshoff Pol. Tract-based analysis of magnetization transfer ratio and diffusion tensor imaging of the frontal and frontotemporal connections in schizophrenia. *Schizophr Bull*, 36(4): 778-87, 2010.

128. Van den Heuvel, M.P., R.C. Mandl, C.J. Stam, R.S. Kahn, and H.E. Hulshoff Pol. Aberrant frontal and temporal complex network structure in schizophrenia: a graph theoretical analysis. *J Neurosci*, 30(47): 15915-26, 2010.

129. Close, T.G., J.D. Tournier, L.A. Johnston, F. Calamante, I. Mareels, and A. Connelly. Fourier Tract Sampling (FouTS): A framework for improved inference of white matter tracts from diffusion MRI by explicitly modelling tract volume. *Neuroimage*, 120: 412-27, 2015.

130. Daducci, A., A. Dal Palu, A. Lemkaddem, and J.P. Thiran. COMMIT: Convex optimization modeling for microstructure informed tractography. *IEEE Trans Med Imaging*, 34(1): 246-57, 2015.

131. Zalesky, A. DT-MRI fiber tracking: a shortest paths approach. *IEEE Trans Med Imaging*, 27(10): 1458-71, 2008.

132. Zalesky, A. and A. Fornito. A DTI-derived measure of cortico-cortical connectivity. *IEEE Trans Med Imaging*, 28(7): 1023-36, 2009.

133. Ercsey-Ravasz, M., N.T. Markov, C. Lamy, D.C. Van Essen, K. Knoblauch, Z. Toroczkai, and H. Kennedy. A predictive network model of cerebral cortical connectivity based on a distance rule. *Neuron*, 80(1): 184-97, 2013.

134. Beul, S.F., S. Grant, and C.C. Hilgetag. A predictive model of the cat cortical connectome based on cytoarchitecture and distance. *Brain Struct Funct*, 220(6): 3167-84, 2015.
135. Roberts, J.A., A. Perry, A.R. Lord, G. Roberts, P.B. Mitchell, R.E. Smith, F. Calamante, and M. Breakspear. The contribution of geometry to the human connectome. *Neuroimage*, 124(Pt A): 379-93, 2016.
136. Van Essen, D.C. and J.H. Maunsell. Two-dimensional maps of the cerebral cortex. *J Comp Neurol*, 191(2): 255-81, 1980.
137. Cottaar, M., S. Jbabdi, M.F. Glasser, K. Dikranian, D.C. Van Essen, T.E. Behrens, and S.N. Sotiropoulos. A Generative Model of White Matter Axonal Orientations Near the Cortex. in *Proceedings of the ISMRM meeting*, Toronto: 351, 2015.
138. St-Onge, E., G. Girard, K. Whittingstall, and M. Descoteaux. Surface tracking from the cortical mesh complements diffusion MRI fiber tracking near the cortex. in *Proceedings of the ISMRM meeting*, Toronto: 2840, 2015.
139. Harwell, J., H. Bremen, O. Coulon, D. Dierker, R.C. Reynolds, C. Silva, K. Teich, D.C. Van Essen, S.K. Warfield, and Z.S. Saad. GIFTI: Geometry data format for exchange of surface-based brain mapping data. in *OHBM Proceedings*, Melbourne, Australia, 2008.
140. Tournier, J.D., C.H. Yeh, F. Calamante, K.H. Cho, A. Connelly, and C.P. Lin. Resolving crossing fibres using constrained spherical deconvolution: validation using diffusion-weighted imaging phantom data. *Neuroimage*, 42(2): 617-25, 2008.
141. Jbabdi, S., S.N. Sotiropoulos, A.M. Savio, M. Grana, and T.E. Behrens. Model-based analysis of multishell diffusion MR data for tractography: How to get over fitting problems. *Magn Reson Med*: doi:10.1002/mrm.24204, 2012.
142. Jeurissen, B., J.D. Tournier, T. Dhollander, A. Connelly, and J. Sijbers. Multi-tissue constrained spherical deconvolution for improved analysis of multi-shell diffusion MRI data. *Neuroimage*, 103: 411-26, 2014.
143. Heidemann, R.M., A. Anwander, T. Feiweier, T.R. Knosche, and R. Turner. k-space and q-space: combining ultra-high spatial and angular resolution in diffusion imaging using ZOOPPA at 7 T. *Neuroimage*, 60(2): 967-78, 2012.
144. McNab, J.A., B.L. Edlow, T. Witzel, S.Y. Huang, H. Bhat, K. Heberlein, T. Feiweier, K. Liu, B. Keil, J. Cohen-Adad, M.D. Tisdall, R.D. Folkerth, H.C. Kinney, and L.L. Wald. The Human Connectome Project and beyond: initial applications of 300 mT/m gradients. *Neuroimage*, 80: 234-45, 2013.
145. Sotiropoulos, S.N., S. Jbabdi, J. Xu, J. Andersson, S. Moeller, E. Auerbach, M.F. Glasser, M. Hernandez, G. Sapiro, M. Jenkinson, D. Feinberg, E. Yacoub, C. Lenglet, D.C. Van Essen, K. Ugurbil, and T.E. Behrens. Advances in diffusion MRI acquisition and processing in the Human Connectome Project. *NeuroImage*, 80: 125-43, 2013.
146. Vos, S.B., M. Aksoy, Z. Han, S.J. Holdsworth, J. Maclaren, M.A. Viergever, A. Leemans, and R. Bammer. Trade-off between angular and spatial resolutions in in vivo fiber tractography. *Neuroimage*, 129: 117-32, 2016.
147. Sotiropoulos, S.N., M. Hernandez-Fernandez, A.T. Vu, J.L. Andersson, S. Moeller, E. Yacoub, C. Lenglet, K. Ugurbil, T.E. Behrens, and S. Jbabdi. Fusion in diffusion MRI for improved fibre orientation estimation: An application to the 3T and 7T data of the human connectome project. *Neuroimage*, 2016.

148.   Reid, A.T., J. Lewis, G. Bezgin, B. Khundrakpam, S.B. Eickhoff, A.R. McIntosh, P. Bellec, and A.C. Evans. A cross-modal, cross-species comparison of connectivity measures in the primate brain. *Neuroimage*, 125: 311-31, 2016.

149.   Calabrese, E., A. Badea, C.L. Coe, G.R. Lubach, M.A. Styner, and G.A. Johnson. Investigating the tradeoffs between spatial resolution and diffusion sampling for brain mapping with diffusion tractography: time well spent? *Hum Brain Mapp*, 35(11): 5667-85, 2014.

150.   Fan, Q., A. Nummenmaa, J.R. Polimeni, T. Witzel, S.Y. Huang, V.J. Wedeen, B.R. Rosen, and L.L. Wald. HIgh b-value and high Resolution Integrated Diffusion (HIBRID) imaging. *Neuroimage*, 150: 162-176, 2017.

151.   St-Jean, S., P. Coupe, and M. Descoteaux. Non Local Spatial and Angular Matching: Enabling higher spatial resolution diffusion MRI datasets through adaptive denoising. *Med Image Anal*, 32: 115-30, 2016.

152.   Veraart, J., D.S. Novikov, D. Christiaens, B. Ades-Aron, J. Sijbers, and E. Fieremans. Denoising of diffusion MRI using random matrix theory. *Neuroimage*, 142: 394-406, 2016.

153.   Alexander, D.C., D. Zikic, A. Ghosh, R. Tanno, V. Wottschel, J. Zhang, E. Kaden, T.B. Dyrby, S.N. Sotiropoulos, H. Zhang, and A. Criminisi. Image quality transfer and applications in diffusion MRI. *Neuroimage*, 152: 283-298, 2017.

154.   Dyrby, T.B., H. Lundell, M.W. Burke, N.L. Reislev, O.B. Paulson, M. Ptito, and H.R. Siebner. Interpolation of diffusion weighted imaging datasets. *Neuroimage*, 103: 202-13, 2014.

155.   Coupe, P., J.V. Manjon, M. Chamberland, M. Descoteaux, and B. Hiba. Collaborative patch-based super-resolution for diffusion-weighted images. *Neuroimage*, 83: 245-61, 2013.

156.   Ugurbil, K., J. Xu, E.J. Auerbach, S. Moeller, A.T. Vu, J.M. Duarte-Carvajalino, C. Lenglet, X. Wu, S. Schmitter, P.F. Van de Moortele, J. Strupp, G. Sapiro, F. De Martino, D. Wang, N. Harel, M. Garwood, L. Chen, D.A. Feinberg, S.M. Smith, K.L. Miller, S.N. Sotiropoulos, S. Jbabdi, J.L. Andersson, T.E. Behrens, M.F. Glasser, D.C. Van Essen, E. Yacoub, and W.U.-M.H. Consortium. Pushing spatial and temporal resolution for functional and diffusion MRI in the Human Connectome Project. *Neuroimage*, 80: 80-104, 2013.

157.   Vu, A.T., E. Auerbach, C. Lenglet, S. Moeller, S.N. Sotiropoulos, S. Jbabdi, J. Andersson, E. Yacoub, and K. Ugurbil. High resolution whole brain diffusion imaging at 7T for the Human Connectome Project. *Neuroimage*, 122: 318-331, 2015.

158.   Moeller, S., E. Yacoub, C.A. Olman, E. Auerbach, J. Strupp, N. Harel, and K. Ugurbil. Multiband multislice GE-EPI at 7 tesla, with 16-fold acceleration using partial parallel imaging with application to high spatial and temporal whole-brain fMRI. *Magn Reson Med*, 63(5): 1144-53, 2010.

159.   Setsompop, K., B.A. Gagoski, J.R. Polimeni, T. Witzel, V.J. Wedeen, and L.L. Wald. Blipped-controlled aliasing in parallel imaging for simultaneous multislice echo planar imaging with reduced g-factor penalty. *Magn Reson Med*, 67(5): 1210-24, 2012.

160.   Shemesh, N., E. Ozarslan, M.E. Komlosh, P.J. Basser, and Y. Cohen. From single-pulsed field gradient to double-pulsed field gradient MR: gleaning new

microstructural information and developing new forms of contrast in MRI. *NMR Biomed*, 23(7): 757-80, 2010.

161. Westin, C.F., H. Knutsson, O. Pasternak, F. Szczepankiewicz, E. Ozarslan, D. van Westen, C. Mattisson, M. Bogren, L.J. O'Donnell, M. Kubicki, D. Topgaard, and M. Nilsson. Q-space trajectory imaging for multidimensional diffusion MRI of the human brain. *Neuroimage*, 135: 345-62, 2016.

162. Andersson, J.L. and S.N. Sotiropoulos. An integrated approach to correction for off-resonance effects and subject movement in diffusion MR imaging. *Neuroimage*, 125: 1063-1078, 2016.

163. Andersson, J.L. and S.N. Sotiropoulos. Non-parametric representation and prediction of single- and multi-shell diffusion-weighted MRI data using Gaussian processes. *Neuroimage*, 122: 166-176, 2015.

164. Graham, M.S., I. Drobnjak, and H. Zhang. Realistic simulation of artefacts in diffusion MRI for validating post-processing correction techniques. *Neuroimage*, 125: 1079-1094, 2016.

165. Irfanoglu, M.O., P. Modi, A. Nayak, E.B. Hutchinson, J. Sarlls, and C. Pierpaoli. DR-BUDDI (Diffeomorphic Registration for Blip-Up blip-Down Diffusion Imaging) method for correcting echo planar imaging distortions. *Neuroimage*, 106: 284-99, 2015.

166. Esteban, O., E. Caruyer, A. Daducci, M. Bach-Cuadra, M.J. Ledesma-Carbayo, and A. Santos. Diffantom: Whole-Brain Diffusion MRI Phantoms Derived from Real Datasets of the Human Connectome Project. *Front Neuroinform*, 10: 4, 2016.

167. Hubbard, P.L., F.L. Zhou, S.J. Eichhorn, and G.J. Parker. Biomimetic phantom for the validation of diffusion magnetic resonance imaging. *Magn Reson Med*, 73(1): 299-305, 2015.

168. Neher, P.F., F.B. Laun, B. Stieltjes, and K.H. Maier-Hein. Fiberfox: facilitating the creation of realistic white matter software phantoms. *Magn Reson Med*, 72(5): 1460-70, 2014.

169. Schmahmann, J.D., D.N. Pandya, R. Wang, G. Dai, H.E. D'Arceuil, A.J. de Crespigny, and V.J. Wedeen. Association fibre pathways of the brain: parallel observations from diffusion spectrum imaging and autoradiography. *Brain*, 130(Pt 3): 630-53, 2007.

170. Lawes, I.N., T.R. Barrick, V. Murugam, N. Spierings, D.R. Evans, M. Song, and C.A. Clark. Atlas-based segmentation of white matter tracts of the human brain using diffusion tensor tractography and comparison with classical dissection. *Neuroimage*, 39(1): 62-79, 2008.

171. Zemmoura, I., B. Serres, F. Andersson, L. Barantin, C. Tauber, I. Filipiak, J.P. Cottier, G. Venturini, and C. Destrieux. FIBRASCAN: a novel method for 3D white matter tract reconstruction in MR space from cadaveric dissection. *Neuroimage*, 103: 106-18, 2014.

172. Martino, J., P.C. De Witt Hamer, F. Vergani, C. Brogna, E.M. de Lucas, A. Vazquez-Barquero, J.A. Garcia-Porrero, and H. Duffau. Cortex-sparing fiber dissection: an improved method for the study of white matter anatomy in the human brain. *J Anat*, 219(4): 531-41, 2011.

173. Martino, J., P.C. De Witt Hamer, M.S. Berger, M.T. Lawton, C.M. Arnold, E.M. de Lucas, and H. Duffau. Analysis of the subcomponents and cortical terminations of the perisylvian superior longitudinal fasciculus: a fiber

dissection and DTI tractography study. *Brain Struct Funct*, 218(1): 105-21, 2013.

174. Martino, J., R. da Silva-Freitas, H. Caballero, E. Marco de Lucas, J.A. Garcia-Porrero, and A. Vazquez-Barquero. Fiber dissection and diffusion tensor imaging tractography study of the temporoparietal fiber intersection area. *Neurosurgery*, 72(1 Suppl Operative): 87-97; discussion 97-8, 2013.

175. Dauguet, J., S. Peled, V. Berezovskii, T. Delzescaux, S.K. Warfield, R. Born, and C.F. Westin. Comparison of fiber tracts derived from in-vivo DTI tractography with 3D histological neural tract tracer reconstruction on a macaque brain. *Neuroimage*, 37(2): 530-8, 2007.

176. Dyrby, T.B., L.V. Sogaard, G.J. Parker, D.C. Alexander, N.M. Lind, W.F. Baare, A. Hay-Schmidt, N. Eriksen, B. Pakkenberg, O.B. Paulson, and J. Jelsing. Validation of in vitro probabilistic tractography. *Neuroimage*, 37(4): 1267-77, 2007.

177. Thomas, C., F.Q. Ye, M.O. Irfanoglu, P. Modi, K.S. Saleem, D.A. Leopold, and C. Pierpaoli. Anatomical accuracy of brain connections derived from diffusion MRI tractography is inherently limited. *Proc Natl Acad Sci U S A*, 111(46): 16574-9, 2014.

178. Azadbakht, H., L.M. Parkes, H.A. Haroon, M. Augath, N.K. Logothetis, A. de Crespigny, H.E. D'Arceuil, and G.J. Parker. Validation of High-Resolution Tractography Against In Vivo Tracing in the Macaque Visual Cortex. *Cereb Cortex*, 25(11): 4299-309, 2015.

179. Knosche, T.R., A. Anwander, M. Liptrot, and T.B. Dyrby. Validation of tractography: Comparison with manganese tracing. *Hum Brain Mapp*, 36(10): 4116-34, 2015.

180. Jbabdi, S., J.F. Lehman, S.N. Haber, and T.E. Behrens. Human and monkey ventral prefrontal fibers use the same organizational principles to reach their targets: tracing versus tractography. *J Neurosci*, 33: 3190-201, 2013.

181. Draganski, B., F. Kherif, S. Kloppel, P.A. Cook, D.C. Alexander, G.J. Parker, R. Deichmann, J. Ashburner, and R.S. Frackowiak. Evidence for segregated and integrative connectivity patterns in the human Basal Ganglia. *J Neurosci*, 28(28): 7143-52, 2008.

182. Scholtens, L.H., M.A. de Reus, and M.P. van den Heuvel. Linking contemporary high resolution magnetic resonance imaging to the von Economo legacy: A study on the comparison of MRI cortical thickness and histological measurements of cortical structure. *Hum Brain Mapp*, 36(8): 3038-46, 2015.

183. Kolasinski, J., C.J. Stagg, S.A. Chance, G.C. Deluca, M.M. Esiri, E.H. Chang, J.A. Palace, J.A. McNab, M. Jenkinson, K.L. Miller, and H. Johansen-Berg. A combined post-mortem magnetic resonance imaging and quantitative histological study of multiple sclerosis pathology. *Brain*, 135(Pt 10): 2938-51, 2012.

184. Gorbach, N.S., C. Schutte, C. Melzer, M. Goldau, O. Sujazow, J. Jitsev, T. Douglas, and M. Tittgemeyer. Hierarchical information-based clustering for connectivity-based cortex parcellation. *Front Neuroinform*, 5: 18, 2011.

185. Tomassini, V., S. Jbabdi, J.C. Klein, T.E. Behrens, C. Pozzilli, P.M. Matthews, M.F. Rushworth, and H. Johansen-Berg. Diffusion-weighted imaging tractography-based parcellation of the human lateral premotor cortex

identifies dorsal and ventral subregions with anatomical and functional specializations. *J Neurosci*, 27(38): 10259-69, 2007.

186. Cerliani, L., R.M. Thomas, S. Jbabdi, J.C. Siero, L. Nanetti, A. Crippa, V. Gazzola, H. D'Arceuil, and C. Keysers. Probabilistic tractography recovers a rostrocaudal trajectory of connectivity variability in the human insular cortex. *Hum Brain Mapp*, 33(9): 2005-34, 2012.

187. Mars, R.B., J. Sallet, U. Schuffelgen, S. Jbabdi, I. Toni, and M.F. Rushworth. Connectivity-based subdivisions of the human right "temporoparietal junction area": evidence for different areas participating in different cortical networks. *Cereb Cortex*, 22(8): 1894-903, 2012.

188. Cloutman, L.L., R.J. Binney, M. Drakesmith, G.J. Parker, and M.A. Lambon Ralph. The variation of function across the human insula mirrors its patterns of structural connectivity: evidence from in vivo probabilistic tractography. *Neuroimage*, 59(4): 3514-21, 2012.

189. Klein, J.C., T.E. Behrens, M.D. Robson, C.E. Mackay, D.J. Higham, and H. Johansen-Berg. Connectivity-based parcellation of human cortex using diffusion MRI: Establishing reproducibility, validity and observer independence in BA 44/45 and SMA/pre-SMA. *Neuroimage*, 34(1): 204-11, 2007.

190. Thiebaut de Schotten, M., M. Urbanski, R. Valabregue, D.J. Bayle, and E. Volle. Subdivision of the occipital lobes: an anatomical and functional MRI connectivity study. *Cortex*, 56: 121-37, 2014.

191. Eickhoff, S.B., S. Jbabdi, S. Caspers, A.R. Laird, P.T. Fox, K. Zilles, and T.E. Behrens. Anatomical and functional connectivity of cytoarchitectonic areas within the human parietal operculum. *J Neurosci*, 30(18): 6409-21, 2010.

192. Zhang, D., A.Z. Snyder, J.S. Shimony, M.D. Fox, and M.E. Raichle. Noninvasive functional and structural connectivity mapping of the human thalamocortical system. *Cereb Cortex*, 20(5): 1187-94, 2010.

193. Johansen-Berg, H., T.E. Behrens, E. Sillery, O. Ciccarelli, A.J. Thompson, S.M. Smith, and P.M. Matthews. Functional-anatomical validation and individual variation of diffusion tractography-based segmentation of the human thalamus. *Cereb Cortex*, 15(1): 31-9, 2005.

194. Lambert, C., L. Zrinzo, Z. Nagy, A. Lutti, M. Hariz, T. Foltynie, B. Draganski, J. Ashburner, and R. Frackowiak. Confirmation of functional zones within the human subthalamic nucleus: patterns of connectivity and sub-parcellation using diffusion weighted imaging. *Neuroimage*, 60(1): 83-94, 2012.

195. Elias, W.J., Z.A. Zheng, P. Domer, M. Quigg, and N. Pouratian. Validation of connectivity-based thalamic segmentation with direct electrophysiologic recordings from human sensory thalamus. *Neuroimage*, 59(3): 2025-34, 2012.

196. Anwander, A., M. Tittgemeyer, D.Y. von Cramon, A.D. Friederici, and T.R. Knosche. Connectivity-Based Parcellation of Broca's Area. *Cereb Cortex*, 17(4): 816-25, 2007.

197. Saygin, Z.M., D.E. Osher, J. Augustinack, B. Fischl, and J.D. Gabrieli. Connectivity-based segmentation of human amygdala nuclei using probabilistic tractography. *Neuroimage*, 56(3): 1353-61, 2011.

198. Bhatia, K.D., L. Henderson, G. Ramsey-Stewart, and J. May. Diffusion tensor imaging to aid subgenual cingulum target selection for deep brain stimulation in depression. *Stereotact Funct Neurosurg*, 90(4): 225-32, 2012.

199. Gutman, D.A., P.E. Holtzheimer, T.E. Behrens, H. Johansen-Berg, and H.S. Mayberg. A tractography analysis of two deep brain stimulation white matter targets for depression. *Biol Psychiatry*, 65(4): 276-82, 2009.

200. Pouratian, N., Z. Zheng, A.A. Bari, E. Behnke, W.J. Elias, and A.A. Desalles. Multi-institutional evaluation of deep brain stimulation targeting using probabilistic connectivity-based thalamic segmentation. *J Neurosurg*, 115(5): 995-1004, 2011.

201. Stephan, K.E., M. Tittgemeyer, T.R. Knosche, R.J. Moran, and K.J. Friston. Tractography-based priors for dynamic causal models. *Neuroimage*, 47(4): 1628-38, 2009.

202. Pineda-Pardo, J.A., R. Bruna, M. Woolrich, A. Marcos, A.C. Nobre, F. Maestu, and D. Vidaurre. Guiding functional connectivity estimation by structural connectivity in MEG: an application to discrimination of conditions of mild cognitive impairment. *Neuroimage*, 101: 765-77, 2014.

203. Honey, C.J., O. Sporns, L. Cammoun, X. Gigandet, J.P. Thiran, R. Meuli, and P. Hagmann. Predicting human resting-state functional connectivity from structural connectivity. *Proc Natl Acad Sci U S A*, 106(6): 2035-40, 2009.

204. Saygin, Z.M., D.E. Osher, E.S. Norton, D.A. Youssoufian, S.D. Beach, J. Feather, N. Gaab, J.D. Gabrieli, and N. Kanwisher. Connectivity precedes function in the development of the visual word form area. *Nat Neurosci*, 19(9): 1250-5, 2016.

205. Cohen, M.X., J.C. Schoene-Bake, C.E. Elger, and B. Weber. Connectivity-based segregation of the human striatum predicts personality characteristics. *Nat Neurosci*, 12(1): 32-4, 2009.

206. Forstmann, B.U., A. Anwander, A. Schafer, J. Neumann, S. Brown, E.J. Wagenmakers, R. Bogacz, and R. Turner. Cortico-striatal connections predict control over speed and accuracy in perceptual decision making. *Proc Natl Acad Sci U S A*, 107(36): 15916-20, 2010.

207. Chowdhury, R., M. Guitart-Masip, C. Lambert, P. Dayan, Q. Huys, E. Duzel, and R.J. Dolan. Dopamine restores reward prediction errors in old age. *Nat Neurosci*, 16(5): 648-53, 2013.

208. Mars, R.B., L. Verhagen, T.E. Gladwin, F.X. Neubert, J. Sallet, and M.F. Rushworth. Comparing brains by matching connectivity profiles. *Neurosci Biobehav Rev*, 60: 90-7, 2016.

209. Neubert, F.X., R.B. Mars, J. Sallet, and M.F. Rushworth. Connectivity reveals relationship of brain areas for reward-guided learning and decision making in human and monkey frontal cortex. *Proc Natl Acad Sci U S A*, 112(20): E2695-704, 2015.

210. Neubert, F.X., R.B. Mars, A.G. Thomas, J. Sallet, and M.F. Rushworth. Comparison of human ventral frontal cortex areas for cognitive control and language with areas in monkey frontal cortex. *Neuron*, 81(3): 700-13, 2014.

211. Sallet, J., R.B. Mars, M.P. Noonan, F.X. Neubert, S. Jbabdi, J.X. O'Reilly, N. Filippini, A.G. Thomas, and M.F. Rushworth. The organization of dorsal frontal cortex in humans and macaques. *J Neurosci*, 33(30): 12255-74, 2013.

212. Croxson, P.L., H. Johansen-Berg, T.E. Behrens, M.D. Robson, M.A. Pinsk, C.G. Gross, W. Richter, M.C. Richter, S. Kastner, and M.F. Rushworth. Quantitative investigation of connections of the prefrontal cortex in the human and macaque using probabilistic diffusion tractography. *J Neurosci*, 25(39): 8854-66, 2005.

213. Rilling, J.K., M.F. Glasser, T.M. Preuss, X. Ma, T. Zhao, X. Hu, and T.E. Behrens. The evolution of the arcuate fasciculus revealed with comparative DTI. *Nat Neurosci*, 11(4): 426-8, 2008.

214. Thiebaut de Schotten, M., F. Dell'Acqua, R. Valabregue, and M. Catani. Monkey to human comparative anatomy of the frontal lobe association tracts. *Cortex*, 48(1): 82-96, 2012.

215. Hecht, E.E., D.A. Gutman, B.A. Bradley, T.M. Preuss, and D. Stout. Virtual dissection and comparative connectivity of the superior longitudinal fasciculus in chimpanzees and humans. *Neuroimage*, 108: 124-37, 2015.

216. Goulas, A., M. Bastiani, G. Bezgin, H.B. Uylings, A. Roebroeck, and P. Stiers. Comparative analysis of the macroscale structural connectivity in the macaque and human brain. *PLoS Comput Biol*, 10(3): e1003529, 2014.

217. Fornito, A., A. Zalesky, and M. Breakspear. Graph analysis of the human connectome: promise, progress, and pitfalls. *Neuroimage*, 80: 426-44, 2013.

218. Van Wijk, B.C., C.J. Stam, and A. Daffertshofer. Comparing brain networks of different size and connectivity density using graph theory. *PLoS One*, 5(10): e13701, 2010.

219. Zalesky, A., A. Fornito, M.L. Seal, L. Cocchi, C.F. Westin, E.T. Bullmore, G.F. Egan, and C. Pantelis. Disrupted axonal fiber connectivity in schizophrenia. *Biol Psychiatry*, 69(1): 80-9, 2011.

220. van den Heuvel, M.P., S.C. de Lange, A. Zalesky, C. Seguin, B.T. Yeo, and R. Schmidt. Proportional thresholding in resting-state fMRI functional connectivity networks and consequences for patient-control connectome studies: Issues and recommendations. *Neuroimage*, 152: 437-449, 2017.

221. Rubinov, M., S.A. Knock, C.J. Stam, S. Micheloyannis, A.W. Harris, L.M. Williams, and M. Breakspear. Small-world properties of nonlinear brain activity in schizophrenia. *Hum Brain Mapp*, 30(2): 403-16, 2009.

222. Alexander-Bloch, A.F., N. Gogtay, D. Meunier, R. Birn, L. Clasen, F. Lalonde, R. Lenroot, J. Giedd, and E.T. Bullmore. Disrupted modularity and local connectivity of brain functional networks in childhood-onset schizophrenia. *Front Syst Neurosci*, 4: 147, 2010.

223. Serrano, M.A., M. Boguna, and A. Vespignani. Extracting the multiscale backbone of complex weighted networks. *Proc Natl Acad Sci U S A*, 106(16): 6483-8, 2009.

224. De Reus, M.A., V.M. Saenger, R.S. Kahn, and M.P. van den Heuvel. An edge-centric perspective on the human connectome: link communities in the brain. *Philos Trans R Soc Lond B Biol Sci*, 369(1653), 2014.

225. Sporns, O. Structure and function of complex brain networks. *Dialogues Clin Neurosci*, 15(3): 247-62, 2013.

226. Van den Heuvel, M.P. and O. Sporns. Rich-club organization of the human connectome. *J Neurosci*, 31(44): 15775-86, 2011.

227. Van den Heuvel, M.P. and O. Sporns. Network hubs in the human brain. *Trends Cogn Sci*, 17(12): 683-96, 2013.

228. Bullmore, E. and O. Sporns. The economy of brain network organization. *Nat Rev Neurosci*, 13(5): 336-49, 2012.

229. Fornito, A., A. Zalesky, and E. Bullmore. Fundamentals of Brain Network Analysis: Academic Press, 2016.

230. Watts, D.J. and S.H. Strogatz. Collective dynamics of 'small-world' networks. *Nature*, 393(6684): 440-2, 1998.

231. Rubinov, M. and O. Sporns. Complex network measures of brain connectivity: uses and interpretations. *Neuroimage*, 52(3): 1059-69, 2010.
232. Kaiser, M. and C.C. Hilgetag. Nonoptimal component placement, but short processing paths, due to long-distance projections in neural systems. *PLoS Comput Biol*, 2(7): e95, 2006.
233. Zalesky, A., A. Fornito, and E.T. Bullmore. Network-based statistic: identifying differences in brain networks. *Neuroimage*, 53(4): 1197-207, 2010.
234. Zalesky, A., A. Fornito, and E. Bullmore. On the use of correlation as a measure of network connectivity. *Neuroimage*, 60(4): 2096-106, 2012.
235. Fornito, A., A. Zalesky, and M. Breakspear. The connectomics of brain disorders. *Nat Rev Neurosci*, 16(3): 159-72, 2015.
236. Raj, A., A. Kuceyeski, and M. Weiner. A network diffusion model of disease progression in dementia. *Neuron*, 73(6): 1204-15, 2012.
237. Zhou, J., E.D. Gennatas, J.H. Kramer, B.L. Miller, and W.W. Seeley. Predicting regional neurodegeneration from the healthy brain functional connectome. *Neuron*, 73(6): 1216-27, 2012.
238. Bassett, D.S. and E. Bullmore. Small-world brain networks. *Neuroscientist*, 12(6): 512-23, 2006.
239. Sporns, O. and R.F. Betzel. Modular Brain Networks. *Annu Rev Psychol*, 67: 613-40, 2016.
240. Dosenbach, N.U., B. Nardos, A.L. Cohen, D.A. Fair, J.D. Power, J.A. Church, S.M. Nelson, G.S. Wig, A.C. Vogel, C.N. Lessov-Schlaggar, K.A. Barnes, J.W. Dubis, E. Feczko, R.S. Coalson, J.R. Pruett, Jr., D.M. Barch, S.E. Petersen, and B.L. Schlaggar. Prediction of individual brain maturity using fMRI. *Science*, 329(5997): 1358-61, 2010.
241. McIntosh, A.R., F.L. Bookstein, J.V. Haxby, and C.L. Grady. Spatial pattern analysis of functional brain images using partial least squares. *Neuroimage*, 3(3 Pt 1): 143-57, 1996.
242. Smith, S.M., T.E. Nichols, D. Vidaurre, A.M. Winkler, T.E. Behrens, M.F. Glasser, K. Ugurbil, D.M. Barch, D.C. Van Essen, and K.L. Miller. A positive-negative mode of population covariation links brain connectivity, demographics and behavior. *Nat Neurosci*, 18(11): 1565-7, 2015.
243. Goni, J., M.P. van den Heuvel, A. Avena-Koenigsberger, N. Velez de Mendizabal, R.F. Betzel, A. Griffa, P. Hagmann, B. Corominas-Murtra, J.P. Thiran, and O. Sporns. Resting-brain functional connectivity predicted by analytic measures of network communication. *Proc Natl Acad Sci U S A*, 111(2): 833-8, 2014.
244. Evans, A.C. Networks of anatomical covariance. *Neuroimage*, 80: 489-504, 2013.
245. Smith, S.M., C.F. Beckmann, J. Andersson, E.J. Auerbach, J. Bijsterbosch, G. Douaud, E. Duff, D.A. Feinberg, L. Griffanti, M.P. Harms, M. Kelly, T. Laumann, K.L. Miller, S. Moeller, S. Petersen, J. Power, G. Salimi-Khorshidi, A.Z. Snyder, A.T. Vu, M.W. Woolrich, J. Xu, E. Yacoub, K. Ugurbil, D.C. Van Essen, M.F. Glasser, and W.U.-M.H. Consortium. Resting-state fMRI in the Human Connectome Project. *Neuroimage*, 80: 144-68, 2013.
246. Toro, R., P.T. Fox, and T. Paus. Functional coactivation map of the human brain. *Cereb Cortex*, 18(11): 2553-9, 2008.
247. Brookes, M.J., M. Woolrich, H. Luckhoo, D. Price, J.R. Hale, M.C. Stephenson, G.R. Barnes, S.M. Smith, and P.G. Morris. Investigating the

electrophysiological basis of resting state networks using magnetoencephalography. *Proc Natl Acad Sci U S A*, 108(40): 16783-8, 2011.

248. Mantini, D., M.G. Perrucci, C. Del Gratta, G.L. Romani, and M. Corbetta. Electrophysiological signatures of resting state networks in the human brain. *Proc Natl Acad Sci U S A*, 104(32): 13170-5, 2007.

249. Van Essen, D.C., S.M. Smith, D.M. Barch, T.E. Behrens, E. Yacoub, K. Ugurbil, and W.U.-M.H. Consortium. The WU-Minn Human Connectome Project: an overview. *Neuroimage*, 80: 62-79, 2013.

250. Glasser, M.F., S.N. Sotiropoulos, J.A. Wilson, T.S. Coalson, B. Fischl, J.L. Andersson, J. Xu, S. Jbabdi, M. Webster, J.R. Polimeni, D.C. Van Essen, M. Jenkinson, and W.U.-M.H. Consortium. The minimal preprocessing pipelines for the Human Connectome Project. *Neuroimage*, 80: 105-24, 2013.

251. De Reus, M.A. and M.P. van den Heuvel. Rich club organization and intermodule communication in the cat connectome. *J Neurosci*, 33(32): 12929-39, 2013.